(12) INTERNATIONAL APPLICATION PUBLISHED UNDER THE PATENT COOPERATION TREATY (PCT)

(19) World Intellectual Property Organization
International Bureau

(43) International Publication Date
10 June 2010 (10.06.2010)

PCT

(10) International Publication Number
WO 2010/063718 A1

(51) **International Patent Classification**:
G01N 33/68 (2006.01) ***C07K 14/705*** (2006.01)
C12N 9/64 (2006.01)

(21) **International Application Number**:
PCT/EP2009/066151

(22) **International Filing Date**:
1 December 2009 (01.12.2009)

(25) **Filing Language**: English

(26) **Publication Language**: English

(30) **Priority Data**:
08020866.3 2 December 2008 (02.12.2008) EP

(71) **Applicant** *(for all designated States except US)*: **ETH ZÜRICH** [CH/CH]; Raemistrasse 101/ETH Transfer, CH-8092 Zürich (CH).

(72) **Inventors; and**
(75) **Inventors/Applicants** *(for US only)*: **STOFFEL, Markus** [DE/CH]; Hochstrasse 6, CH-8044 Zurich (CH). **ESTERHAZY, Daria** [AT/CH]; Furkastrasse 18, CH-8044 Zurich (CH). **AEBERSOLD, Rudolf** [CH/CH]; Wiesenrain 15, CH-8049 Zurich (CH). **KREK, Wilhelm** [AT/CH]; Wiesenrain 15, CH-8704 Herrliberg (CH).

(74) **Agent**: **KUENG, Peter**; F.Hoffmann - La Roche AG, Grenzacherstrasse 124, CH-4070 Basel (CH).

(81) **Designated States** *(unless otherwise indicated, for every kind of national protection available)*: AE, AG, AL, AM, AO, AT, AU, AZ, BA, BB, BG, BH, BR, BW, BY, BZ, CA, CH, CL, CN, CO, CR, CU, CZ, DE, DK, DM, DO, DZ, EC, EE, EG, ES, FI, GB, GD, GE, GH, GM, GT, HN, HR, HU, ID, IL, IN, IS, JP, KE, KG, KM, KN, KP, KR, KZ, LA, LC, LK, LR, LS, LT, LU, LY, MA, MD, ME, MG, MK, MN, MW, MX, MY, MZ, NA, NG, NI, NO, NZ, OM, PE, PG, PH, PL, PT, RO, RS, RU, SC, SD, SE, SG, SK, SL, SM, ST, SV, SY, TJ, TM, TN, TR, TT, TZ, UA, UG, US, UZ, VC, VN, ZA, ZM, ZW.

(84) **Designated States** *(unless otherwise indicated, for every kind of regional protection available)*: ARIPO (BW, GH, GM, KE, LS, MW, MZ, NA, SD, SL, SZ, TZ, UG, ZM, ZW), Eurasian (AM, AZ, BY, KG, KZ, MD, RU, TJ, TM), European (AT, BE, BG, CH, CY, CZ, DE, DK, EE, ES, FI, FR, GB, GR, HR, HU, IE, IS, IT, LT, LU, LV, MC, MK, MT, NL, NO, PL, PT, RO, SE, SI, SK, SM, TR), OAPI (BF, BJ, CF, CG, CI, CM, GA, GN, GQ, GW, ML, MR, NE, SN, TD, TG).

Declarations under Rule 4.17:

— *of inventorship (Rule 4.17(iv))*

Published:

— *with international search report (Art. 21(3))*

— *with sequence listing part of description (Rule 5.2(a))*

WO 2010/063718 A1

(54) **Title**: SCREENING ASSAY FOR METABOLIC DISEASE THERAPEUTICALS

(57) **Abstract**: The present invention relates to a screening assay for the identification of compounds for the treatment of metabolic disorders.

Screening assay for metabolic disease therapeuticals

The present invention relates to a screening assay for the identification of compounds for the treatment of metabolic disorders.

Defective glucose – stimulated insulin secretion and decreased β - cell mass are the main causes of hyperglycemia in type 2 diabetes mellitus. The transmembrane protein Tmem27 (Collectrin) is expressed in pancreatic β-cells where it regulates pancreatic β -cell mass, and insulin secretion. Tmem27 is inactivated at the plasma membrane by proteolytic cleavage and shedding.

BACE1 is a β-secretase (β-site of APP cleaving enzyme), belongs to the class of aspartic acid proteases and has been implicated in the pathogenesis of Alzheimer disease and in the formation of myelin sheaths in peripheral nerve cells. It is a transmembrane proteins, contains two active site aspartate residues in its extracellular protein domain and may function as a dimmer.

The generation of the 40 or 42 amino acid long amyloid β -proteins that aggregate in the brain of Alzheimer's patients requires two sequential cleavages of the amyloid precursor protein (APP). Extracellular cleavage of APP by BACE releases a soluble extracellular fragment and is followed by APP cleavage within its transmembrane domain by γ-secretase (presenilin). The second cleavage releases the intracellular domain of APP and amyloid-β. Since α-secretase cleaves APP closer to the cell membrane than BACE does, it removes a fragment of the amyloid- β peptide. Initial cleavage of APP by an α-secretase rather than BACE prevents eventual generation of amyloid-β.

Unlike APP and the presenilin proteins important in γ -secretase, no known mutations in the gene encoding BACE cause the early-onset, familial Alzheimer's disease. However, levels of this enzyme have been shown to be elevated in Alzheimer's. The

physiological purpose of BACE's cleavage of APP and other transmembrane proteins is unknown. BACE2 is a close homolog of BACE1.

The aim of the present invention was to provide a new target for the identification of compounds for the treatment of metabolic disorders.

The inventors of the present invention have identified BACE2 as the protease cleaving Tmem27. Inhibition of BACE2 leads to inhibition of Tmem27 shedding and an increase of the full length protein.

The present invention provides a screening assay for identifying modulators (including stimulators and inhibitors) of the ability of BACE2 to cleave Tmem27 resulting in the modulation (e.g. suppression) of Tmem27 cleavage. BACE2, and Tmem27, can be present in isolated, immobilized or cell bound form or in the form of membrane-enzyme mixture, are contacted with a candidate compound, or a plurality of candidate compounds, and those candidates are selected that alter, preferably inhibit, BACE2-mediated cleavage of Tmem27 protein. The effect of a candidate compound on BACE2 activity is preferably detected by monitoring its ability to alter (e.g. reduce) the amount of cleaved Tmem27. Both cell-free and cell based assays, including assays performed with cell membrane-enzyme preparations are specifically within the scope of the invention.

In a preferred embodiment, the assay involves contacting Tmem27 and BACE2 as individual components or as a mixture or complex with a test compound, and thereafter determining the level of soluble product of Tmem27 proteolysis. The Tmem27 and BACE2 which are contacted with the compound can be both isolated from cell membranes obtained from cells expressing both Tmem27 and BACE2 or can be isolated from cells expressing either Tmem27 or BACE and then combined together. Alternatively, Tmem27 and/or BACE2 may be partially or fully synthesized by traditional chemical synthesis and/or recombinant DNA technology.

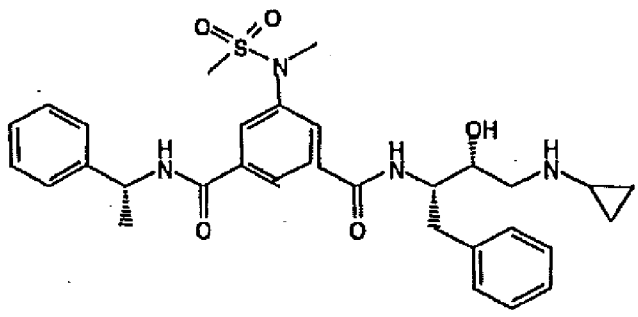
In a further preferred embodiment, cells engineered to recombinantly express BACE2 and Tmem27 can be used. For example, following incubation of cells expressing BACE2 and Tmem27 with the test compound, the supernatant is assayed for levels of soluble products of Tmem27 proteolysis. Detection of Tmem27 proteolytic products can be accomplished using any of a number of methods to determine the absence or presence or altered amounts of the expressed polypeptide in the test sample. In general, antibodies that specifically bind a polypeptide of the invention are added to a sample, and incubated for a period of time sufficient to allow binding to the epitope. The antibody can be detectably labeled for direct detection (e.g., using radioisotopes, enzymes, fluorescers, chemiluminescers, and the like), or can be used in conjunction with a second stage

antibody or reagent to detect binding (e.g., biotin with horseradish peroxidase-conjugated avidin, a secondary antibody conjugated to a fluorescent compound, e.g., fluorescein, rhodamine, Texas Red, etc.). Any suitable alternative method of qualitative or quantitative detection of levels or amounts of differentially expressed polypeptide can be used, for example western blot, immunoprecipitation, radioimmunoassay, etc. In a particular embodiment, an enzyme-linked immunosorbent assay (ELISA) is used to detect the presence of the Tmem27 proteolytic products. Quantitation of multiple samples can be made more time efficient by running the assay in an ELISA format for rapid quantitation by spectrophotometric or colorimetric detection.

In a further preferred embodiment of the inventive assay, the Tmem27 polypeptide is a fusion polypeptide comprising a transmembrane domain, a BACE2 cleavage site and a compound or peptide having a detectable readout. The cleaved and released Tmem27 peptide can be detected using an established method for detecting the compound or peptide having a detectable readout. Preferred compounds with a detectable readout are flurorophores and GFP.

In a preferred embodiment of the method of the present invention, the BACE2 cleavage site of the fusion polypeptide comprises a peptide having the amino acid sequence disclosed in Seq. Id. No. 2.

In another object, the present invention relates to the use of a compound having the formula 1 (Merck BI= compound A) for the manufacture of a medicament for the treatment of a metabolic disease, preferably type II diabetes. Formula 1:



The term "Tmem27" is used herein to refer to native sequence Tmem27 from any animal, e.g. mammalian, species, including humans, and Tmem27 variants. The Tmem27 polypeptides may be isolated from a variety of sources, including human tissue types or prepared by recombinant and/or synthetic methods.

"Native sequence Tmem27" refers to a polypeptide having the same amino acid sequence as a Tmem27 polypeptide occurring in nature regardless of its mode of preparation. A native sequence Tmem27 may be isolated from nature, or prepared by recombinant and/or synthetic methods. The term "native sequence Tmem27" specifically encompasses naturally occurring truncated or secreted forms, naturally occurring variant forms (e.g. alternatively spliced forms), and naturally occurring allelic variants of Tmem27. The identifier of the human Tmem27 polypeptide in the swissprot database is Q9HBJ8 (Seq. Id. No. 1).

The term "Tmem27 variant" refers to amino acid sequence variants of a native sequence Tmem27, containing one or more amino acid substitution and/or deletion and/or insertion in the native sequence. The amino acid sequence variants generally have at least about 75%, preferably at least about 80%, more preferably at least about 85%, even more preferably at least about 90%, most preferably at least about 95% sequence identity with the amino acid sequence of a native sequence Tmem27. The term “Tmem27 variant” refers as well to Tmem27 fragments which can be processed by BACE2 e.g. truncated Tmem27 polypeptides which are still a substrate for BACE2.

The term "BACE2" is used herein to refer to native sequence BACE2 from any animal, e.g. mammalian, species, including humans, and BACE2 variants (which are further defined below). The BACE2 polypeptides may be isolated from a variety of sources, including human tissue types or prepared by recombinant and/or synthetic methods.

"Native sequence BACE2" refers to a polypeptide having the same amino acid sequence as a BACE2 polypeptide occurring in nature regardless of its mode of preparation. A native sequence BACE2 may be isolated from nature, or prepared by recombinant and/or synthetic methods. The term "native sequence BACE2" specifically encompasses naturally occurring truncated or secreted forms, naturally occurring variant forms (e.g. alternatively spliced forms), and naturally occurring allelic variants of BACE2. The identifier of the human BACE2 polypeptide in the swissprot database is Q9Y5Z0.

The term "BACE2 variant" refers to amino acid sequence variants of a native sequence BACE2, containing one or more amino acid substitution and/or deletion and/or insertion in the native sequence. The amino acid sequence variants generally have at least about 75%, preferably at least about 80%, more preferably at least about 85%, even more preferably at least about 90%, most preferably at least about 95% sequence identity with the amino acid sequence of a native sequence BACE2.

The term "compound" is used herein in the context of a "test compound" or a "drug candidate compound" described in connection with the assays of the present invention. As such, these compounds comprise organic or inorganic compounds, derived synthetically or from natural sources. The compounds include inorganic or organic compounds such as polynucleotides, lipids or hormone analogs that are characterized by relatively low molecular weights. Other biopolymeric organic test compounds include peptides comprising from about 2 to about 40 amino acids and larger polypeptides comprising from about 40 to about 500 amino acids, such as antibodies or antibody conjugates.

Short description of the figures

Figure 1 shows supernatant (SN) to cell lysate ratios of expression levels of Tmem27 in the presence of the indicated protease inhibitor;

Figure 2A shows Relative levels of shed Tmem27 from Min6 cells following inhibition of specific protease inhibitors using RNAi;

Figure 2B shows expression levels of shed Tmem27 from Min 6 cells treated with control siRNAs (siControl and siTmem27) and pool si12 (targeting Bace2);

Figure 3A shows that BACE1 silencing has no effect on Tmem27 cleavage;

Figure 3B shows steady state mRNA levels of BACE1 and BACE2 using Affimetrix expression arrays;

Figure 3C shows an immunoblot of MIN6 cells transfected with different siRNAs targeting BACE1 (A-F) or controls (siControl, siBACE2) using anti BACE1 antibodies;

Figure 4A shows relatedness of different proteases based on amino acid sequence;

Figure 4B shows different Cathepsins expressed in MIN6 cells;

Figure 5 shows that lack of cleavage stabilizes full-length Tmem27;

Figure 6 shows efficient knock-down of cathepsins in MIN6 cells treated with respective siRNA pool;

Figures 7A-C show that overexpression of BACE1 and BACE2 destabilizes Tmem27 and increases shedding from MIN6 cells;

Figure 8 shows that overexpression of BACE1 and BACE2 destabilizes Tmem27 and increases shedding from HEK293 cells; expression levels of BACE1, BACE2 and Tmem27 were measured in total cell lysates;

Figures 9A-B show that overexpression of BACE1 and BACE2 destabilizes Tmem27 and increases shedding from HEK293 cells; expression levels of shed Tmem27 were measured in supernatants;

Figures 10A-B show that pharmacological inhibition of BACE mimics the effect of siRNA against BACE2;

Figure 11 shows inhibitor concentration dependence of Tmem27 shedding;

Figure 12 shows that MerckBI inhibitor decreases Tmem27 shedding in mouse islets;

Figure 13 shows that peptide hTmem27-C inhibits Tmem27 shedding;

Figure 14 shows that peptide hTmem27-C inhibits Tmem27 shedding more efficiently than non-stabilized OM003; and

Figure 15 shows reciprocal regulation of BACE1 and BACE2 in mutant null mice and stabilization of Tmem27.

Fig. 16 show pharmacological inhibition of Bace2 and its effects on Tmem27 levels and MIN6 proliferation.

Fig. 16A: Quantification of shed Tmem27 in the supernatant of MIN6 cells treated with various BACE inhibitors (n=3).

Fig. 16B: Western blot for Tmem27, Bace1 and Bace2 in MIN6 cell lysate after treatment with various BACE inhibitors.

Fig. 16C: Quantification of shed Tmem27 in the supernatant of murine islets treated with various BACE inhibitors (n=4).

Fig. 16D: Western blot for Tmem27 and Bace2 in murine islet lysate after treatment with MerckBI

Data represent means ± s.d. *$P \leq 0.05$; **$P \leq 0.01$;***$P \leq 0.001$ by one-tailed Student's t test for unpaired data (a, c).

Fig. 17 shows stabilisation of the C-terminal fragment (CTF) of Tmem27 and identification of its cleavage sites

Fig. 17 A: Western blot for Tmem27 in MIN6 cell lysate upon treatment with gamma sectretase inhibitor S2188

Fig. 17B: Western blot for TMEM27 in cell lysates from MIN6 expressing either hTMEM27del 171-222V5 or hTMEM27V5

Fig. 17C: Mass spectra of Tmem27 peptides found in the digest of the hTMEM27del 171-222V5 CTF (left) and hTMEM27del 171-222V5 (right).

Fig. 17D: Mass spectra of Tmem27 peptides found in the digest of the supernatant from MIN6 cells stably expressing pcDNA, pBACE2 or pBACE2 D93A,D303A(B2DM).

Fig. 17E: Amino acid sequence of the Tmem27 cleavage site region with peptides identified highlighted

Fig. 17F: Alignment of the Tmem27 cleavage site region from different species and comparison to other reported Bace2 cleavage sites

Fig. 18 shows validation of Bace2 as the Tmem27 protease in vivo

Fig. 18A: Western blot for Tmem27 and Bace2 in MIN6 cell lysate after transfection with plasmids encoding wild type (WT) BACE2, BACE2 ΔE6, BACE2D303A or BACE2 D93A.

Fig. 18B: Western blot for Tmem27 and Bace2 in CL and SN of isolated islets from Bace2ΔE6/ΔE6 mice and WT littermates

Fig. 18C: Western blot for Tmem27, Bace1 and Bace2 in CL and SN of isolated islets from Bace1-/- mice and WT littermates

Fig. 18D: Western blot for Tmem27 in kidney protein extracts from Bace2ΔE6/ΔE6 , Bace1-/- , and WT littermates

Fig. 19 shows localisation of Bace2 to non-insulin granules in the pancreatic beta cell

Fig. 19A: 0x images of murine islets stained for Bace2 and insulin, glucagon, somatostatin and pancreatic polypeptide (PP)

Fig. 19B: 63 x image of a murine beta cell stained for Bace2 and insulin

Fig. 19C: 40x image of murine islets stained for Bace2 and Tmem27

Fig. 19E: 10-70% sucrose gradient of subcellular fractions from MIN6 cells

Fig. 20 shows quantitative PCR analysis of steady state mRNAs of Bace1, Bace2 and Tmem27 in mouse tissues. Indicated are relative levels.

Fig. 21 shows improved blood glucose handling and increased beta cell mass in Bace2ΔE6/ΔE6 mice

Fig. 21A: ad libitum fed blood glucose levels of Bace2ΔE6/ΔE6 and Bace2+/+ mice (n=10-12)

Fig. 21B: Blood glucose levels before (0 min) and after an intraperitoneal glucose injection (5-120 min) of Bace2ΔE6/ΔE6 and Bace2+/+ mice (n=10)

Fig. 21C: Serum insulin levels of Bace2ΔE6/ΔE6 and Bace2+/+ mice after a 6h fast (0 min) and after an intraperitoneal glucose injection(n=12)

Fig. 21D: Percentage of starting blood glucose level reached by Bace2ΔE6/ΔE6 and Bace2+/+ mice (n=10) after an intraperitoneal insulin injection

Fig. 21E: Insulin release by isolated islets from Bace2ΔE6/ΔE6 and Bace2+/+ mice incubated at indicated glucose concentrations (n=3)

Fig. 21F: Total insulin content of pancreata from Bace2ΔE6/ΔE6 and Bace2+/+ mice (n=5-7)

Fig. 21G: Beta cell mass of Bace2ΔE6/ΔE6 and Bace2+/+ mice (n=3).Mass was calculated by multiplying percentage of beta cell positive surface area by pancreatic wet weight

Fig. 21H: Percentage of Ki-67 positive beta cell nuclei in Bace2ΔE6/ΔE6 and Bace2+/+ pancreata (n=5)

Data represent means ± s.d. *P ≤ 0.05; **P ≤ 0.01;***P ≤ 0.001 by one-tailed Student's t test for unpaired data

Experimental Part

Protease inhibitor screen identifies Cathepsin family/aspartyl proteases as class of enzyme cleaving TMEM27

Fig. 1 shows supernatant (SN) to cell lysate ratios of expression levels of Tmem27 in the presence of the indicated inhibitor. Confluent MIN6 in 24 well plates cells were pre-incubated with 100 μM Protease inhibitor in triplicates for 2 hrs, followed by replacement of OptiMEM medium with fresh medium containing the same inhibitor concentration and further culturing for 3 hrs before supernatant and cell lysate was collected. Tmem27 concentrations in the medium were then assayed by immunoblotting and quantitation using Kodak densitometry software. The ratio of shed to full-length TMEM27 was decreased by

protease inhibitors (known targets in brackets) 11=E-64 (Calpain; Cathepsins, Papain), 15=Enalapril (ACE), 19=Z-FA-FMK (Cathepsins B, L, S), 26=MDL-28170 (Calpain, Cathepsin B), 28=TLCK (Trypsin like serine proteases), 34=CA-74 (Cathepsin B), 35=AAF-CMK (Tripeptidyl peptidase3), 39=Arphamenine B (Aminopeptidase3), 52=Nafamostat mesylate (Tryptase).

Relative levels of shed Tmem27 from Min6 cells following inhibition of specific protease inhibitors using RNAi.

Fig. 2A: Min 6 cells were transfected with 1 μM siRNA pool targeting 29 proteases expressed in MIN6 cell. After 12 hrs, the medium was changed to OptiMEM, the supernatant was collected for the last 24 hrs after transfection and analyzed by semiquantitative immunoblotting using an anti-Tmeme27 antibody. Signal intensities were quantified by densitometry using Kodak imaging software. A scrambled siRNA pool (siControl) and a siRNA targeting Tmem27 were used as controls. All pools consisted of 4 siRNAs (Dharmacon/Fisher). All assays were performed in duplicates.

Fig. 2B: Validation experiment. Expression levels of shed Tmem27 from Min 6 cells treated with control siRNAs (siControl and siTmem27) and pool si12 (targeting Bace2).

No effect of Tmem27 cleavage in Min6 cells as a result of silencing Bace1 by RNA interference

Fig. 3A: Min 6 cells were transfected with 1 μM RNAi pool targeting 29 proteases expressed in MIN6 cell. After 12 hrs, the medium was changed to OptiMEM, the supernatant was collected for the last 24 hrs after transfection and analyzed by semiquantitative immunoblotting using an anti-Tmeme27 antibody. Signal intensities were quantified by densitometry using Kodak imaging software. A scrambled siRNA pool (siControl) and a siRNA targeting Bace2 were used as controls.

Fig. 3B: Steady state mRNA levels in MIN6 cells using Affymetrix expression arrays. Probe intensities indicate that both Bace 1 and 2 are expressed, with Bace-2 being the predominant Bace.

Fig. 3C: Immunoblot of MIN6 cells transfected with different siRNAs targeting Bace1(A-F) or controls (siComtrol, siBace2) using anti Bace-1 antibodies.

Structurally related proteases have no effect on Tmem27 cleavage

Fig. 4A: Diagram showing relatedness of different proteases based on amino acid sequence.

Fig. 4B: Diagram showing different Cathepsin expressed in Min 6 cells, as determined by Affymetrix gene expression analysis.

Fig. 4C: Amino acid sequence alignment showing structural relationship between Bace 1 and Bace 2.

Lack of cleavage stabilizes full-length Tmem27

Fig. 5: Western blots showing increased expression levels of full-length Tmem27 in cell lysates of Min6 cells that were transfected with 4 different siRNAs targeting Bace2 (siBace 1-4), a pool of 4 siRNAs targeting Bace2 (Pool), a scrambled control siRNA (siControl) and siRNA pools targeting Cathepsin L (CTSL), Cathepsin B (CTSB), Cathepsin E (CTS E), Cathepsin F (CTSF), Cathepsin H (CTSH) and Bace 1 (siBace1). Min 6 cells were transfected with 1 μM RNAi in MIN6 cell. Total cell lysates were prepared 36 hrs after transfection and analyzed by immunoblotting using an anti-Tmem27 antibody.

Efficient knock-down of cathepsins in Min6 cells treated with respective siRNA pool.

Fig. 6: Expression levels of Cathepsin B (CTSB), Cathepsin D (CTSD), Cathepsin Z (CTS Z), Cathepsin H (CTSH), Cathepsin L (CTSL) and Cathepsin F (CTSF) in presence and absence of respective siRNAs. Min 6 cells were transfected with 1 μM RNAi in MIN6 cell. Total RNA was prepared 36 hrs after transfection and analyzed by quantitative RT-PCR.

Overexpression of Bace 1 and 2 destabilizes Tmem27 and increases shedding from MIN6 cells

Fig. 7A: Expression levels measured of Tmem27, Bace 1 and Bace 2 measured by immunoblotting after tranfection with expression vectors of human Bace 1 (pDEAT12.2Bace 1), human Bace 2 (pDEST12.2.BACE2, pXL4-BACE2), empty expression vector (pcDNA3) or a vector expressing GFP. Both Bace 2 and to a lesser degree Bace 1 destabilized Tmem27. Min 6 cells were transfected with the indicated expression vectors and total cell lysates were prepared 80 hrs after transfection and analyzed by immunoblotting using an anti-C-terminal Tmem27, Bace1 and Bace2 antibodies.

Fig. 7B: Expression levels of shed Tmem27 measured by immunoblotting of cognate supernatants for the last 48hrs before harvesting with expression vectors of human Bace-1 (pDEAT12.2Bace 1), human Bace-2 (pDEST12.2.BACE2, pXL4-BACE2), empty

expression vector (pcDNA3) or a vector expressing GFP using anti-N-terminal Tmeme27 antibody.

Fig. 7C: Validation experiment. Expression levels of shed Tmem27 measured by immunoblotting of cognate supernatants for the last 48hrs before harvesting with expression vectors of human Bace-1 (pDEAT12.2Bace 1), human Bace-2 (pDEST12.2.BACE2, pXL4-BACE2), empty expression vector (pcDNA3) or a vector expressing GFP using anti-N-terminal Tmeme27 antibody. Increased levels of cleaved Tmeme27 can be observed in supernatants of Bace-1 and Bace-2 transfected MIN6 cells.

Overexpression of Bace 1 and 2 destabilizes Tmem27 and increases shedding in HEK293 cells

Fig. 8: Hek293 cells, which do not express Bace 1, 2 and Tmem27 were transfected with constant amounts of a vector expressing hHA-Tmem27V5 and increasing amounts of vectors of human Bace 1 (pDEAT12.2Bace 1) or human Bace 2 (pDEST12.2.BACE2, pXL4-BACE2). Amount of DNA used per transfection was adjusted by complementing with empty expression vector (pcDNA3). Expression levels of Tmem27, Bace 1 and Bace 2 were measured 80 hrs after transfection in total cell lysates using anti V5, Bace 2 or Bace 1 antibodies. Both Bace 2 and Bace 1 destabilized Tmem27.

Overexpression of Bace-1 and Bace-2 increases shedding of Tmem27 in Hek293 cells

Fig. 9A: Hek293 cells, which do not express Bace-1, -2 and Tmem27 were transfected with constant amounts of a vector expressing hHA-Tmem27V5 and increasing amounts of vectors of human Bace-1 (pDEAT12.2Bace 1) or human Bace-2 (pDEST12.2.BACE2, pXL4-BACE2). Amount of DNA used per transfection was adjusted by complementing with empty expression vector (pcDNA3). Expression levels of shed Tmem27 was measured in supernatants by immunoblotting and quantitation using Kodak densitometry software.

Fig. 9B: Tmem27 expression in supernatants of Bace-1 and Bace-2 co-transfected cells were measured for the last 48 hrs after transfection using an anti HA antibody.

Pharmacological inhibition of Bace mimics the effect of siRNA against Bace 2 (= prevention of cleavage and stabilisation of FLTMEM27)

Fig. 10A: Confluent MIN6 in 24 well plates cells were preincubated with Bace inhibitors at the indicated concentrations for 2 hrs, followed by replacement of OptiMEM medium with fresh medium containing the same inhibitor concentration and further

culturing for 24 hrs before supernatant was collected. Tmem27 concentrations in the medium were then assayed by immunoblotting and quantitation using Kodak densitometry software. Significant decreases in the levels of Tmeme27 were observed in supernatants of OM-992, OM-003 and MerckBI treated Min6 cells.

Fig. 10B: Confluent MIN6 in 24 well plates cells were preincubated with Bace inhibitors at the indicated concentrations for 2 hrs, followed by replacement of OptiMEM medium with fresh medium containing the same inhibitor concentration and further culturing for 24 hrs before cells were harvested and total cell extracts were prepared. Tmem27 concentrations in the cell extracts were then assayed by immunoblotting using anti-Tmem27 antibody. Significant increases in the levels of full length Tmeme27 were observed Min6 cells treated with inhibitors OM-992, OM-003 and MerckBI.

Inhibitor concentration dependence of Tmem27 shedding

Fig. 11: Confluent MIN6 in 24 well plates cells were pre-incubated with Bace inhibitors at the increasing concentrations for 2 hrs, followed by replacement of OptiMEM medium with fresh medium containing the same inhibitor concentration and further culturing for 24 hrs before supernatant was collected. Tmem27 concentrations in the medium were then assayed by immunoblotting and quantitation using Kodak densitometry software. Significant decreases in the levels of Tmeme27 were observed in supernatants of OM-992, OM-003 and MerckBI treated Min6 cells. IC50 Merck BI=150nM, IC50 OM-003= 500 nM.

MerckBI inhibitor (compound A) decreases Tmem 27 shedding in mouse islets

Fig. 12: Mouse islets were isolated by retrograde collagenase perfusion, Histopaque gradient centrifugation and hand picking. Islets were cultured o/n and 50 islets were treated with indicated inhibitor or carrier (DMSO) in a 24 well plate and 450 µl OptiMEM for 48 h. The indicated dose was added after 0 and 24 h. Tmem27 concentrations in the medium were then assayed by immunoblotting and quantitation using Kodak densitometry software. A significant decrease in the levels of Tmeme27 was observed in supernatants of MerckBI treated pancreatic islets.

Peptide hTmem27-C inhibits Tmem27 shedding

Fig. 13: Confluent MIN6 in 24 well plates cells were pre-incubated for 2hrs with 100 µM peptides based on Tmem27 sequence only (H, I, 107,114), chimaeras between Tmem27 and APP (A-G), 2.5 µM OM-003 or carrier (DMSO), followed by exchange to fresh 450 µl OptiMEM with respective peptide for 1.5hrs. Tmem27 concentrations in the medium were then assayed by immunoblotting and quantitation using Kodak densitometry

software. A significant decrease in the levels of Tmem27 was observed in supernatants of peptide C treated cells.

Peptide hTmeme27-C inhibits Tmem27 shedding more efficiently than none-stabilized OM003

Fig. 14: Confluent MIN6 in 24 well plates cells were pre-incubated for 2 hrs with increasing concentrations of peptide C or none-stabilized OM-003 (N-ELDLAAEF-C), 2.5 µM OM-003 or carrier (DMSO), followed by exchange to fresh 450 µl OptiMEM with respective peptide for 1.5hrs. Tmem27 concentrations in the medium were then assayed by immunoblotting. A significant decrease in the levels of Tmem27 was observed in supernatants of 50 and 100 µM peptide C treated cells.

Reciprocal regulation of Bace-1 and Bace-2 in mutant null mice and stabilization of Tmeme27

Fig. 15: Pancreatic islets of wildtype (C57/Bl6) and mutant Bace 1 (Bace 1–/–) and Bace 2 (Bace 2–/–) mice were isolated and expression of Bace-1, Bace-2 and full-length Tmem27 was analyzed by immunoblotting using specific antibodies. Increased expression of Bace-1 in Bace-2–/– mice and of Bace-2 in Bace-1–/– mice can be observed, suggesting that the loss of expression of a particular Bace can be partially compensated. Furthermore, full-length Tmem27 is increased in cell lysates of Bace-1–/– and Bace-2–/– mice. Anti-□-tubulin antibodies were used as a loading control.

Stabilization of TMEM27 by BACE inhibitors

Compounds A (MerckBI), B and C stabilize full length TMEM27, lead to the BACE2 prodomain shift, and the loss of shed TMEM27 in the supernatant of MIN6 cells. Compound A not only leads to a loss of shed TMEM27 in the supernatant of isolated islets, but also the prodomain shift of BACE2 and the stabilization of TMEM27 in the islet cell lysate.

To obtain proof of principle if pharmacological inhibition of Bace2 can affect Tmem27 expression we tested none-selective BACE inhibitors in vitro. MIN6 cells were incubated in the presence of various BACE inhibitors and the levels of shed and full-length Tmem27 were monitored. Most of the BACE inhibitors led to a substantial loss of the Tmem27 ectodomain in the supernatant and accumulation of full-length Tmem27 in cell lysates, respectively (Fig. 16A, B), indicating that Bace2 was efficiently inhibited by these inhibitors. Notably, the Bace2 antibody detected a second higher molecular weight band in the lysates of cells treated with effective inhibitors (Fig. 16B), which has been described as the 'prodomain shift'. Since Bace2 removes its prodomain autocatalytically, this indicates

that an intracellular location is the site of action by which the inhibitors block the zymogen. Consistently, inhibitors showing no activity towards Bace2 in MIN6 cells (APP Sta-Val, ROCHE BI, compound D) share the feature of not being able to penetrate the cell membrane (Fig. 16B). We also tested if BACE inhibitors are effective in primary pancreatic b-cells. Mouse islets were incubated with the two most potent BACE inhibitors and Tmem27 was measured in the culture medium and cell lysates (Fig. 16C). Although higher doses of the inhibitor were needed, the Merck BACE inhibitor (Merck BI) had the same effect on Tmem27 and Bace2 in isolated islets as in MIN6 cells: Tmem27 shedding into the culture medium was reduced, full-length Tmem27 was stabilized, and about 50% of the Bace2 protein displayed the prodomain shift (Fig. 16C, D). These data demonstrate that cell-permeable BACE inhibitors represent an alternative tool to inactivate Bace2 and to stabilize Tmem27 in vivo and that the Bace2 prodomain shift can be used as an indicator for the activity of BACE inhibitors.

Identification of TMEM27 cleavage sites by Bace 2

The previously described Bace1 and Bace2 substrates are structurally diverse type I transmembrane proteins that are subject to a second intramembrane cleavage at hydrophobic Bace cleavage sites carried out by the gamma secretase complex. In order to establish the extent to which Tmem27 behaves like a canonical Bace1/2 substrate, we sought to determine whether the C-terminal fragment (CTF) of Tmem27 was also a substrate of the gamma secretase complex and if the Bace2 cleavage site showed homology to known substrates. To this end, MIN6 cells were incubated with gamma secretase inhibitor S2188 and cell lysates were analyzed by western blotting. The 22 kDa band was detected by the anti-C-Tmem27 antibody in the cell lysate (Fig. 17A) that corresponded to the CTF previously observed only when Tmem27 was overexpressed.These data show that the CTF of Tmem27 is a substrate of gamma secretase.

For mapping the Bace2 cleavage site of Tmem27, two complementary approaches were taken, one to identify the starting point of the CTF, and one to determine the end of the shed fragment of Tmem27. To enrich for the CTF, MIN6 cells overexpressing TMEM27 with a shortened cytosolic tail (TMEM27- Δ171-222-V5) were incubated with a gamma secretase inhibitor (DAPT). The 17 kDa CTF was isolated (Fig.17B), digested by trypsin and analyzed by mass spectrometry. Two peptides corresponding to the cleavage sites were identified, one starting with F117 (site I), one starting with N119 (site II), and these peptides were not detected in a full lengthTMEM27 control sample (Fig. 17C, E). To map the end of the shed part of Tmem27, the supernatant of MIN6 cells was collected, subjected to tryptic digest and then analyzed by mass spectrometry. A peptide ending at F125 was detected (site III, Fig.17 D,E), and this peptide was also highly enriched in the supernatant when BACE2 was overexpressed in MIN6 cells, indicating that site III is a true

BACE2 cleavage site as well (Fig.17D). While site III was not seen in the CTF tryptic digest because the resulting L126-K127 dipeptide is very short and therefore probably lost during sample preparation, the peptides ending at sites I and II could not be observed in the digest of the shed Tmem27 due to the lack of charged residues. These three TMEM27 cleavage sites are relatively conserved amongst different species (Fig.17F) and resemble described alpha-secretase sites, which can be grouped into sites where cleavage occurs between a Leu and an Ala/Asp/Asn residue (Fig.17F, in red) and sites cleaved between Phe and a hydrophobic residue (Fig.17F, in blue). Furthermore, the existence of multiple proximal cleavage sites is common amongst Bace substrates, and so together, these data demonstrate that the proteolytic processing of Tmem27 follows the common pattern of alpha secretase substrates, which are first cleaved at hydrophobic sites in the ectodomain and subsequently turned over by gamma secretase.

Stable BACE2 expressing MIN6 line generation and supernatant preparation for Mass spectrometry

Stable MIN6 cell lines were generated by transfection with the pBACE2 and pBACE2 DM plasmids and selection with 380 mg/ml G418 (Calbiochem). For supernatant analysis, the stable cell lines were cultured in Opti-MEM (Invitrogen) for 24 h. The medium was collected and spun to remove cell debris. The supernatant was concentrated using Amicon Ultra-15 Centrifugal Filter Units with a 10,000-molecular-weight cutoff (Amicon; Millipore, Bedford, MA) and purified by multiple washing steps with 2M Urea 0.1 mM Ammoniumbicarbonate buffer. The disulfide bonds were reduced by tris(2-carboxyethyl) phosphine at a final concentration of 5 mM at 37 °C for 1 h and the free cysteines were alkylated with 0.4 M iodoacetamide at room temperature for 30 minutes in the dark. The alkylation was terminated by adding 0.5 M N-acetylcysteine and incubation for 15 minutes at room temperature. The proteins were digested with sequencing grade modified trypsin (Promega, Madison, Wisconsin) at 1 µg/200 µg of supernatant protein overnight at 37 °C. The peptides were cleaned up as described above and 1/10 of the sample was utilized for each LC-MS/MS experiment .

Mass spectrometric analysis

The setup of the nano liquid chromatography (LC)-MS system was as described previously (Schmidt et al, MCP, 2008). The hybrid LTQ-FT-Ultra-ICR mass spectrometer was interfaced to a nanoelectrospray ion source (both Thermo Electron, Bremen, Germany) coupled online to a Tempo 1D-plus nanoLC (Applied Biosystems/MDS Sciex, Foster City, CA). Peptides were separated on a RP-LC column (75 µm x 15 cm) packed in-house with C18 resin (Magic C18 AQ 3 µm; Michrom BioResources, Auburn, CA, USA) using a linear gradient from 98% solvent A (98% water, 2% acetonitrile, 0.15% formic acid) and

2% solvent B (98% acetonitrile, 2% water, 0.15% formic acid) to 30% solvent B over 40 minutes at a flow rate of 0.3 µl/min. Precursor selection for triggering MS/MS scans from the survey scan acquired in the ICR-cell at 100,000 FWHM was carried out using a combination of data-dependent acquisition of the two most intense ions followed by directed MS-sequencing of all possible fragments of the peptides "NRINNAFFLNDQTLEFLK" (Seq. Id. No. 2) . In detail, the exact precursor ion masses of all possible peptide fragments were calculated for charge states 2, 3 and 4 and subjected to inclusion list driven MS-sequencing as recently specified (Schmidt et al, MCP, 2008). The range of the survey scans was adjusted to the fragment ion masses and reaching from 125 to 1250 m/z. Charge state screening was employed to select for ions with at least two charges and rejecting ions with undetermined charge state. The normalized collision energy was set to 32%, and one microscan was acquired for each spectrum. The mass spectrometric analysis of the peptide mixtures derived from the cell supernatant was carried out as described above using standard data-dependent acquisition of the three most intense precursor ions.

Data analysis

MS/MS spectra were searched using the BIOWORKS search tool [Yates, 1995, Analytical Chem.] against a decoy database (consisting of forward and reverse protein sequences) of the predicted mouse proteome (IPI database, v3.26). The search was performed with semi-lys-C cleavage specificity and 1 missed cleavage site allowed, mass tolerance of 10 ppm, methionine oxidation as variable modification and cysteine carbamidomethylation as fixed modification. The database search results were further filtered and the peptide false discovery rate (FDR) was set to 1%.

For quantification, the extracted ion chromatograms (XICs) for the peptides confidently identified and assigned to the surface protein TMEM27 were generated by the Qual Browser software (Thermo, Bremen, Germany) and finally the corresponding areas calculated and compared. The peptide "GNSADIQHSGGRSSLEGPRFEGK" (Seq. Id. No. 3) was employed as a reference to normalize for variations in TMEM27 peptide amounts analyzed by LC-MS/MS.

For the normalization of the cleaved peptide "INSAFFLDDHTLEF" (Seq. Id. No. 4) detected in the supernatant media, the peak areas of all identified proteins were determined and aligned over all samples using the SuperHirn algorithm (Mueller L., et al. Proteomcis, 2007). Based on these intensities, relative protein abundance ratios were calculated between samples and used to normalize for variations in sample amounts.

The Bace2 ko (delta E6, Bace2ΔE6/ΔE6) mouse not only has stabilized TMEM27 in the cell lysate of islets, but this also correlates with loss of shed TMEM27. (BACE2 Delta E6 overexpression does not lead to Tmem27 destabilization, showing the protease is catalytically inactive)

Because the BACE inhibitors ablating Bace2 activity in isolated islets were not selective for Bace2, we could not rule out a contribution to Tmem27 shedding by Bace1 or other related aspartyl proteases in primary pancreatic beta cells. To substantiate the evidence that Bace2 is the main protease cleaving Tmem27 in vivo, mice with an in-frame deletion of exon 6 of Bace2 on one allele (Bace2ΔE6/ΔE6) were used for further studies. The deletion of exon 6, an exon that encodes 30 amino acids including the Asp303 residue, can be predicted to impair the catalytic activity of Bace2. To test this, wildtype and Bace2ΔE6 mutation were expressed in MIN6 cells and the effect on Tmem27 stabilization was measured. As shown in Fig. 18A, the Bace2ΔE6 mutation abolished the Tmem27 destabilizing effect of overexpressing wildtype Bace2, partly because this truncation of Bace2 led to lowered Bace2 protein stability, but mainly due to the catalytic inactivation, since a single point mutation of Asp303 to Ala303, which did not affect Bace2 protein expression levels, resulted in the ablation of BACE2 activity and lack of Tmem27 cleavage (Fig. 18A). Therefore, the lack of exon 6 in Bace2 results in a fully inactive Bace2 protein.

Bace2ΔE6/ΔE6 mice also have stabilized TMEM27, but concomitantly an increase in shed TMEM27 that reflects the higher TMEM27 levels. BACE2 levels are unaltered, as are Tmem27 and Bace2 mRNA levels

To unambiguously exclude the possibility that Bace1 participates in Tmem27 processing, the same experiment was performed with islets of Bace1–/– mice and wildtype littermates. Intriguingly, the Tmem27 levels in Bace1–/– islet lysates were augmented with respect to wildtype lysates as well (Fig. 18C). However, because the Tmem27 ectodomain in the supernatant was equally elevated, whilst the Bace2 levels were unchanged (Fig. 18C), this increase of Tmem27 appeared to be independent of direct cleavage and rather a consequence of altered beta cell function or islet composition in Bace1–/– mice.

BACE2 is only expressed in the beta cell within the pancreas, in compartment distinct from insulin granules, co-localizing with the plasma membrane proteins E-Cadherin and Tmem27.

To determine the site of Bace2 presence within the islet, pancreatic sections where co-stained for Bace2 and insulin, glucagon, somatostatin, and pancreatic polypeptide (PP), as markers for beta, alpha, delta and PP cells, respectively. Bace2 signals were solely obtained from insulin-positive cells, indicating that the only site of Bace2 protein

expression in the pancreas is the beta cell (Fig. 19A). Bace2 appeared to reside in intracellular vesicles mainly, that were however distinct from insulin granules, as the stainings were non-overlapping (Fig. 19B). Pancreatic sections were also stained for Bace2 and Tmem27, and the two proteins co-localized (Fig. 19C). To confirm that the compartment of Bace2 and Tmem27 co-localization was the plasma membrane and its associated vesicles, MIN6 cell membrane fractions were separated on a sucrose gradient (Fig. 19D). Both Tmem27 and Bace2 peaked with E-cadherin, a cell surface protein, and this peak was distinct from the main insulin containing fraction that marked the insulin granule, suggesting that the main site of co-existence of Tmem27 and Bace2 is the plasma membrane and vesicles derived from it. Together, the data show that Bace2 is a beta-cell enriched protease and that Tmem27 is a beta cell specific substrate.

Expression levels are highest in the islet, followed by stomach and colon. Overall, the protein expression profile is more stringent than the published mRNA expression profile.

Bace2 mRNA has previously been reported to be present in multiple tissues, including the pancreas and kidney, the two main sites of Tmem27 expression. We therefore interrogated if the Bace2 mRNA correlated with Bace2 protein expression in these tissues. Protein extracts were prepared from the 17 organs/tissues in which Bace2 mRNA has been observed and analyzed by western blotting. Contrary to the mRNA expression in these organs, the Bace2 protein was not detected in any CNS structure or the kidney, but was confined to ovaries, colon, and most prominently pancreatic islets (Fig. 20).

Bace2ΔE6/ΔE6 mice have lower random fed blood glucose levels than WT littermates from adulthood on, and show improved glucose tolerance in an IPGTT that is progressive with age.

Overexpression of Tmem27 in the beta cell leads to beta cell expansion and improved glucose homeostasis. It was therefore intriguing to hypothesize that the absence of active Bace2, which stabilizes and increases Tmem27 levels, might lead to metabolic effects. Plasma glucose levels of ad libitum fed Bace2ΔE6/ΔE6 mice and wildtype littermate controls were monitored up to the age of 17 weeks. Bace2ΔE6/ΔE6 animals displayed persistently reduced random fed blood glucose levels from the age of about 8 weeks on (Fig. 21A). No changes in body weight were measured in the two genotypes (data not shown). To investigate if Bace2ΔE6/ΔE6 animals exhibited an improved performance in a hyperglycemic setting, the two groups were challenged with an intraperitoneal glucose tolerance test. Bace2ΔE6/ΔE6 mice displayed lower blood glucose levels throughout the 2 h interval following the injection compared to the wildtype mice (Fig. 21B), indicating that these mice clear glucose from the circulation more efficiently. Increased insulin sensitivity of Bace2ΔE6/ΔE6 mice was ruled out by an insulin tolerance test, in which mutant and

control animals behaved similarly (Fig. 21C), and by contrast, plasma insulin levels after a 6h fast and 15 minutes after a glucose injection were increased in Bace2ΔE6/ΔE6 compared to control mice (Fig. 21D).. Since additionally, isolated Bace2ΔE6/ΔE6 islets secreted more insulin when exposed to physiological levels of glucose than did size matched islets from wild type mice (Fig. 21D), the improved glucose tolerance observed was in part explained by an increased secretory capacity of Bace2ΔE6/ΔE6 islets.

Bace2ΔE6/ΔE6 exhibit increased pancreatic beta cell mass

In order to test if inactivation of Bace2 also has an effect on pancreatic b-cell growth we measured the total pancreatic insulin content and the beta cell mass in Bace2ΔE6/ΔE6and control mice. Pancreatic insulin content was increased in Bace2ΔE6/ΔE6 mice (Fig. 21F), however, no changes were measured for glucagon. The pancreatic beta cell mass approximately doubled in pancreata of Bace2ΔE6/ΔE6 animals compared to wildtype littermates (Fig. 21G), while the mass of other islet cell types was not changed (data not shown). To establish whether the increased beta cell mass was due to accelerated beta cell proliferation, the percentage of Ki67 positive cells was determined (Fig. 21H). Since Bace2ΔE6/ΔE6 mice had twice as many Ki67-positive beta cells, the increase in b-cell mass is most likely to due to increase in b-cell proliferation. Taken together, Bace2ΔE6/ΔE6mice exhibit an improved glucose homeostasis that correlates not only with the raised Tmem27 levels, but also with increased insulin secretory capacity of islets and augmented beta cell proliferation and mass. Therefore, the metabolic phenotype of Bace2ΔE6/ΔE6 mice demonstrates that inactivation of Bace2 is beneficial for b-cell function.

Amino acid sequences

Protein/Peptide	**Disclousre**	**Seq. Id. No.**
Human Tmem27	p. 3	Seq. Id. No. 1
NRINNAFFLNDQTLEFLK	p.15 and Fig. 17C	Seq. Id. No. 2
GNSADIQHSGGRSSLEGPRFEGK	p. 16	Seq. Id. No. 3
INSAFFLDDHTLEF	p. 16	Seq. Id. No. 4
RMNKRINNAFFLNDQTLEFLKIPSLAPPMD PSVPI	Fig. 17F	Seq. Id. No. 5
RKNRNRINSAFFLDDHTLEFLKIPSTLAPP MEPSVPV	Fig. 17F	Seq. Id. No. 6

RMNRNRINNAFFLNDQTLEFLRIPSTLAPP TDPSVPI	Fig. 17F	Seq. Id. No. 7
RNERNRINSAFLLDDKTLEFVQIPPTLAPA TQTSSSS	Fig. 17F	Seq. Id. No. 8
RQSKHRINNAFLLSDMTLEFVGVPPTLAVP IQYNTPP	Fig. 17F	Seq. Id. No. 9
PAERHADGLA LAEPALASPA GAANFLAMVD	Fig. 17F	Seq. Id. No. 10
SEVLDAEFRHDSGYEVHHQKLVFFAEDVGS NK	Fig. 17F	Seq. Id. No. 11
SEVKMDAEFRHDSGYEVHHQKLVFFAEDVG SNK	Fig. 17F	Seq. Id. No. 12
LEVVHNTLSFQTLRTTVKEA SSTFS	Fig. 17F	Seq. Id. No. 13
RMNKNRINNAFFLNDQTLEF LKIPSTLAPP	Fig. 17E	Seq. Id. No. 14
RKNRNRINSAFFDDHTLEFL KIPSTLAPP	Fig. 17E	Seq. Id. No. 15
NDQTLEFLK	Fig. 17C	Seq. Id. No. 16
FLNDQTLEFLK	Fig. 17C	Seq. Id. No. 17

While there are shown and described presently preferred embodiments of the invention, it is to be distinctly understood that the invention is not limited thereto but may be otherwise variously embodied and practiced within the scope of the following claims.

Claims

1. A method for identifying compounds for the treatment of a metabolic disorder comprising: contacting a BACE2 polypeptide and a Tmem27 polypeptide with a compound and determining whether the compound modulates BACE2 mediated Tmem27 cleavage.

2. The method of claim 1, wherein the method is a cell based assay.

3. The method of claim 2, wherein the cell comprises genetic constructs expressing the BACE2 peptide and the Tmem27 peptide.

4. The method of claims 2 to 3, wherein Tmem27 cleavage is determined by measuring cleaved TMEM27 polypeptide in the supernatant.

5. The method of claims 1 to 4, wherein the Tmem27 polypeptide is a fusion polypeptide with a compound or peptide having a detectable readout, preferably a fluorescent readout.

6. The method of claims 1 to 5, wherein the Tmem27 polypeptide is a fusion polypeptide which comprises a transmembrane region, a BACE2 cleavage site and a compound having a detectable readout.

7. The method of claim 6, wherein the the BACE2 cleavage site of the fusion polypeptide comprises a peptide having the amino acid sequence disclosed in Seq. Id. No. 2.

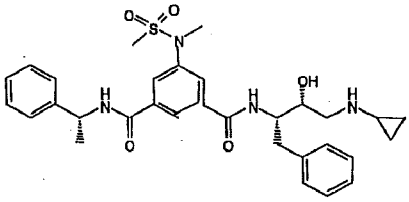
8. The method of claims 1 to 5, wherein the TMEM27 peptide is a full length Tmem27 peptide.

9. The method of claims 1 to 8, wherein the metabolic disorder is diabetes, preferably type 2 diabetes.

10. Use of a BACE 2 peptide for the identification of compounds for the treatment of a metabolic disorder, preferably diabetes, more preferably type 2 diabetes.

11. Use of a compound having formula 1 for the manufacture of a medicament for the treatment of a metabolic disease, preferably type II diabetes.

Formula 1:



11. The methods and compounds as essentially described hereinbefore.

Fig. 1

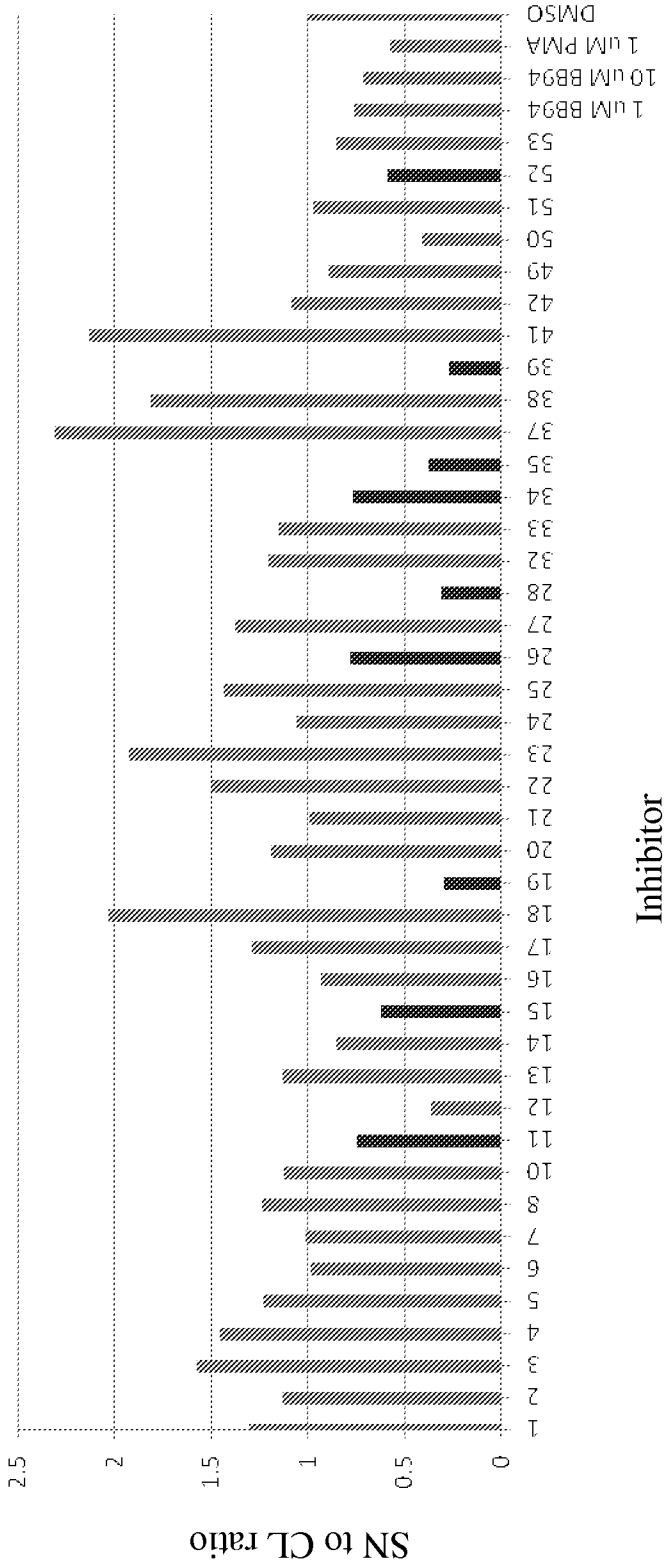
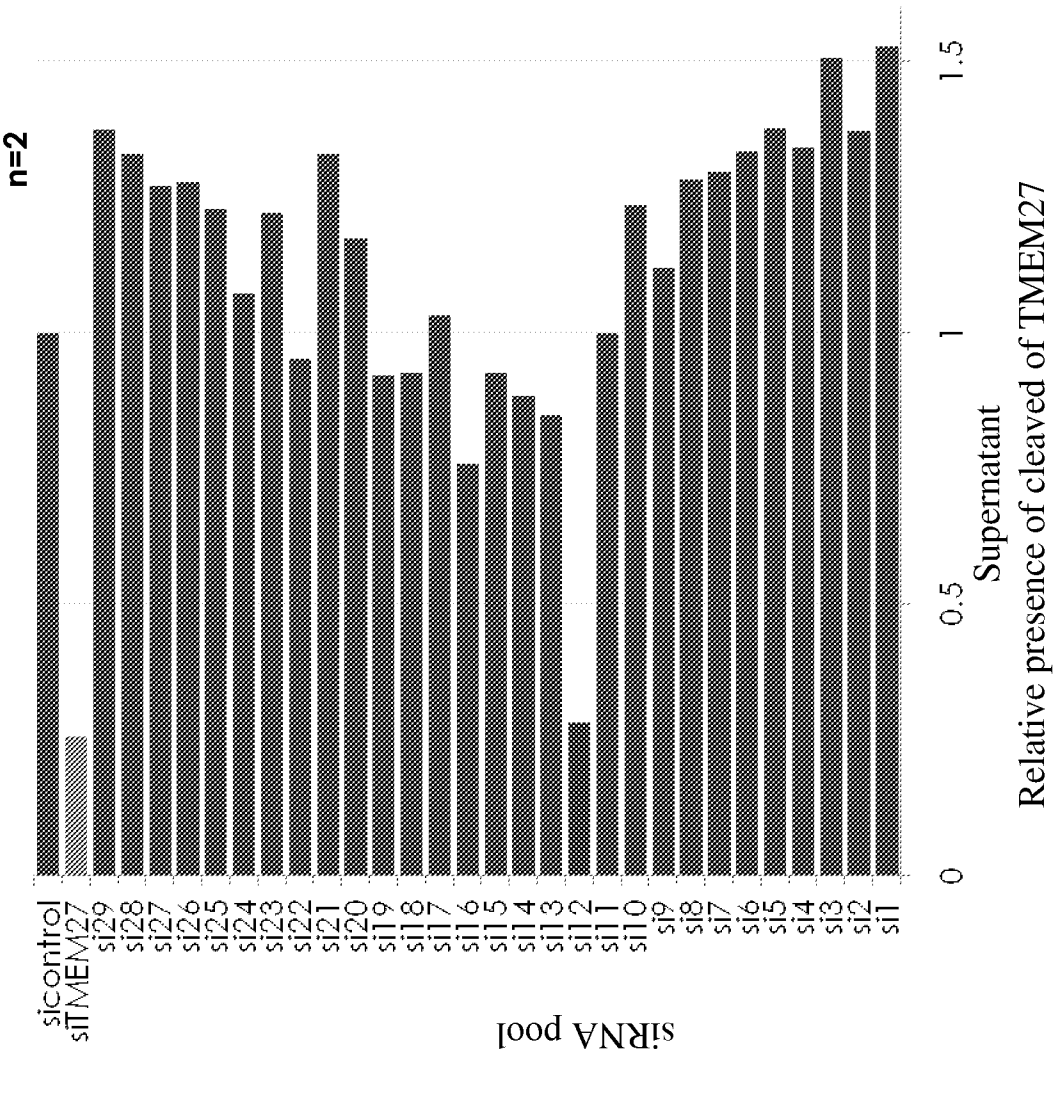

Protease inhibitor screen
SN to CL ratio
2.5
2
1.5
1
0.5
0
Inhibitor
1
2
3
4
5
6
7
8
10
11
12
13
14
15
16
17
18
19
20
21
22
23
24
25
26
27
28
32
33
34
35
37
38
39
41
42
49
50
51
52
53
1 uM BB94
10 uM BB94
1 uM PMA
DMSO

Fig. 2A.


n=2
sicontrol
siTMEM27
si29
si28
si27
si26
si25
si24
si23
si22
si21
si20
si19
si18
si17
si16
si15
si14
si13
si12
si11
si10
si9
si8
si7
si6
si5
si4
si3
si2
si1
siRNA pool
0
0.5
1
1.5
Supernatant
Relative presence of cleaved of TMEM27

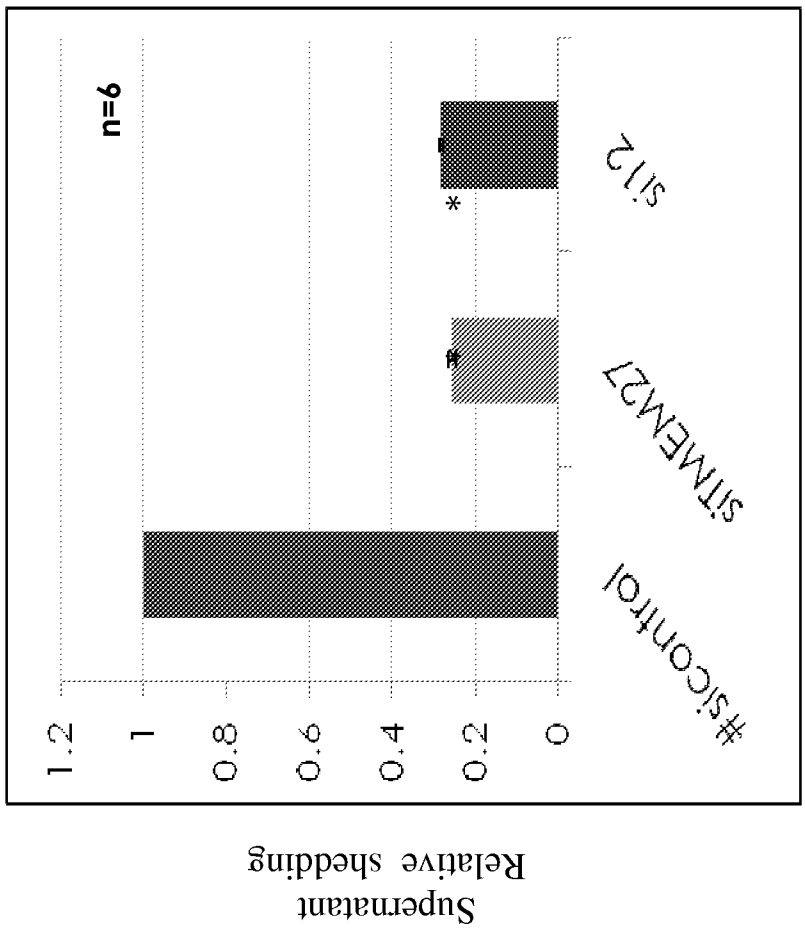

Supernatant
Relative shedding
1.2
1
0.8
0.6
0.4
0.2
0
n=6
*
#
#siControl
siTMEM27
si12

Fig. 2B.

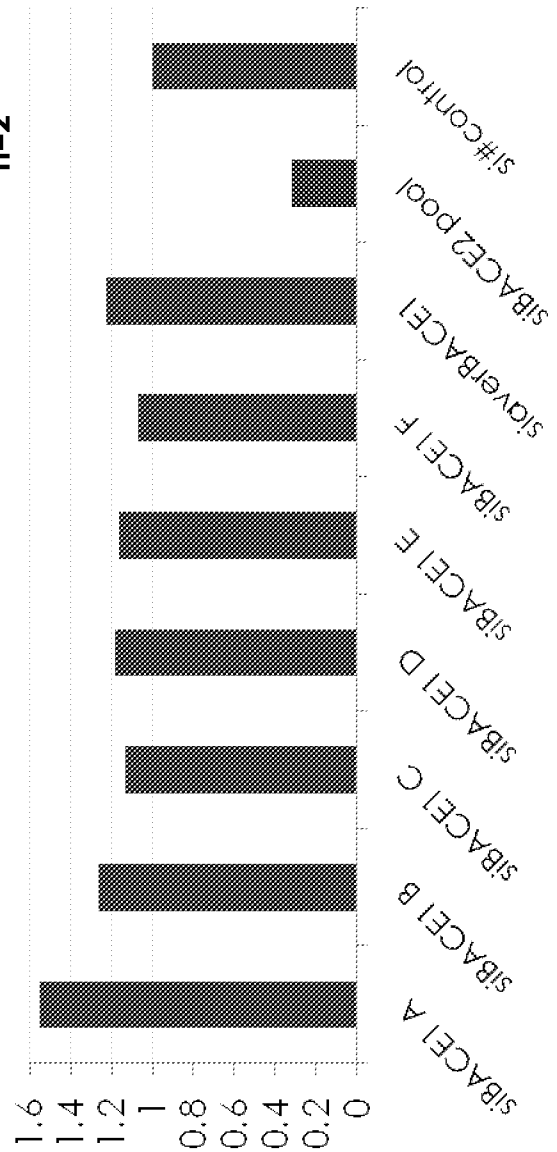

n=2
Relative TMEM27 in supernatant
1.6
1.4
1.2
1
0.8
0.6
0.4
0.2
0
siBACE1 A
siBACE1 B
siBACE1 C
siBACE1 D
siBACE1 E
siBACE1 F
siOverBACE1
siBACE2 pool
si#control

Fig. 3A

Fig. 3B

Affymetrix™

	GFP- Signal	pValue
BACE2	4379.5	2.4E-04
	1731.9	5.9E-03
	966.3	1.4E-02
BACE1	614	1.9E-02
	419.1	1.9E-02
	243	2.4E-04
	191	2.4E-04

Fig. 3C

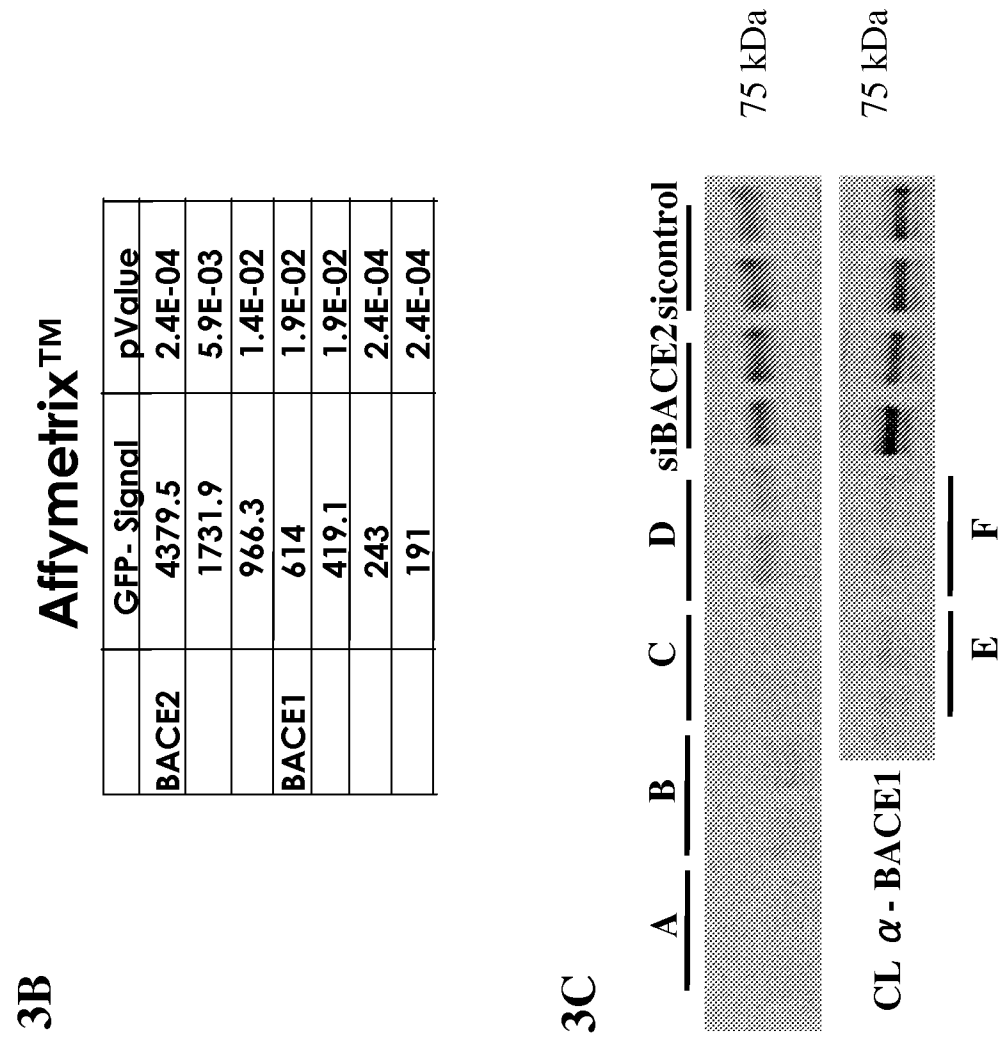


Fig. 4A.

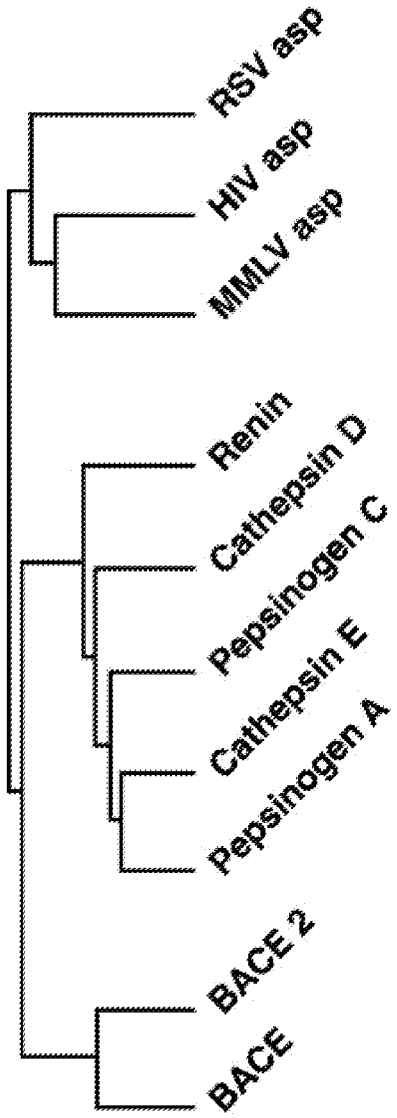


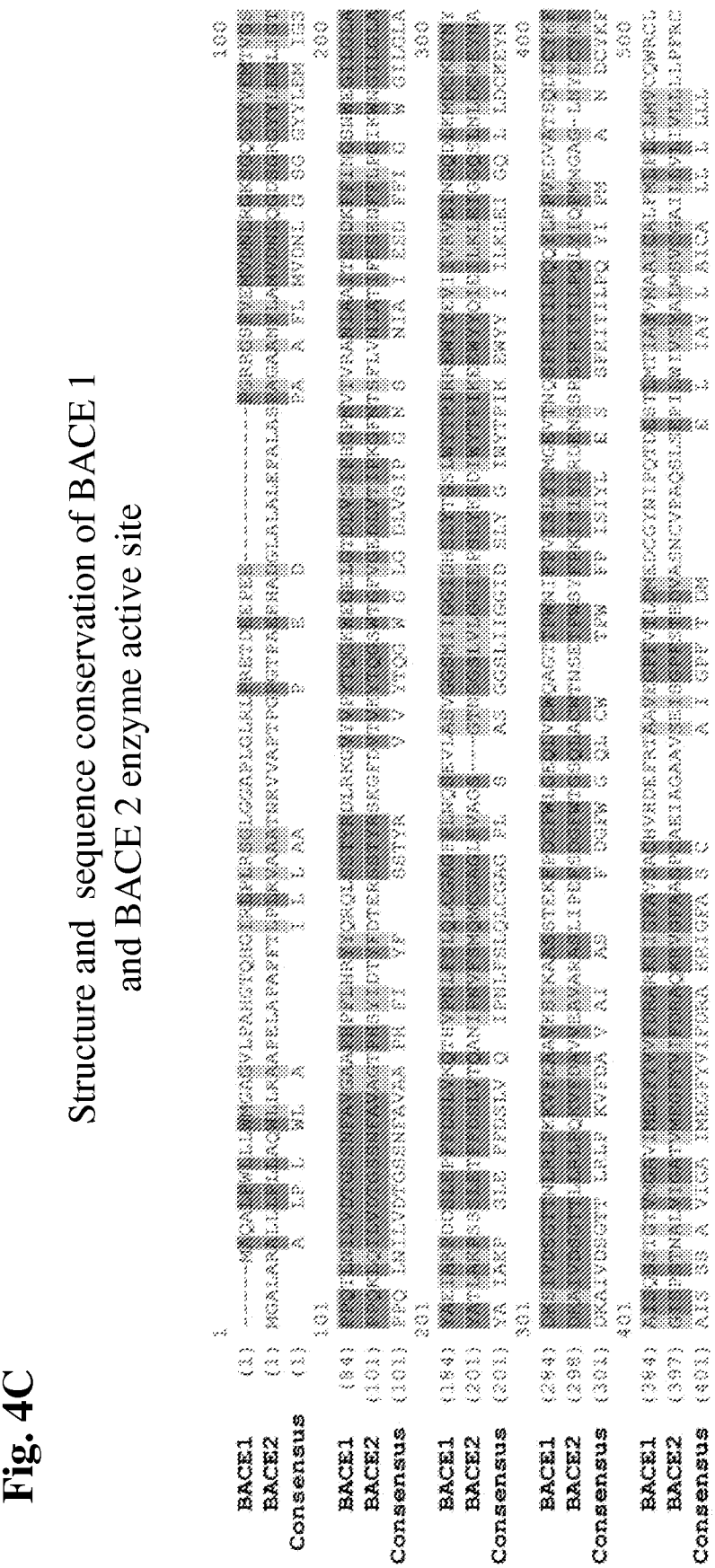
Fig. 4B.

Expressed in MIN6:

Cathepsin B	Cathepsin L
Cathepsin D	Cathepsin Z
Cathepsin E	Bace 1
Cathepsin F	Bace2
Cathepsin H	

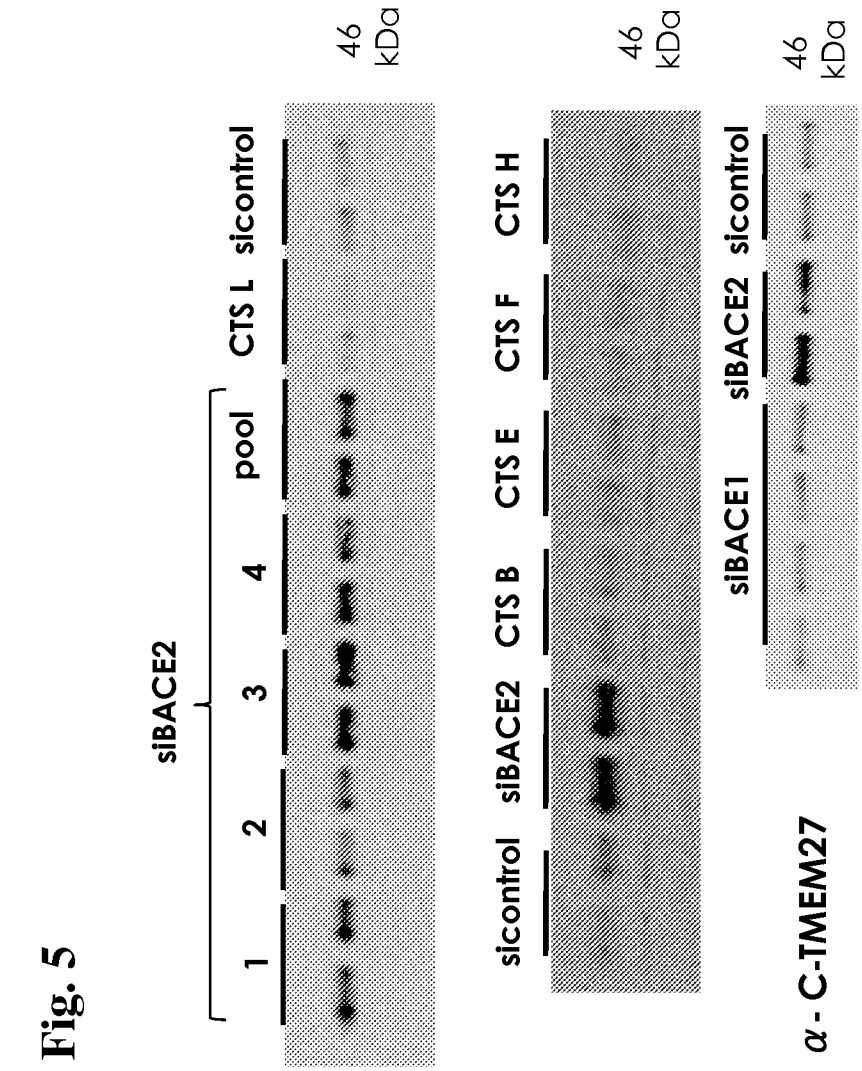
Fig. 4C

Structure and sequence conservation of BACE 1 and BACE 2 enzyme active site



From Chou, Journal of Proteome Research 2004

Fig. 5


siBACE2
1
2
3
4
pool
CTS L
sicontrol
46 kDa
sicontrol
siBACE2
CTS B
CTS E
CTS F
CTS H
46 kDa
siBACE1
siBACE2
sicontrol
46 kDa
α - C-TMEM27

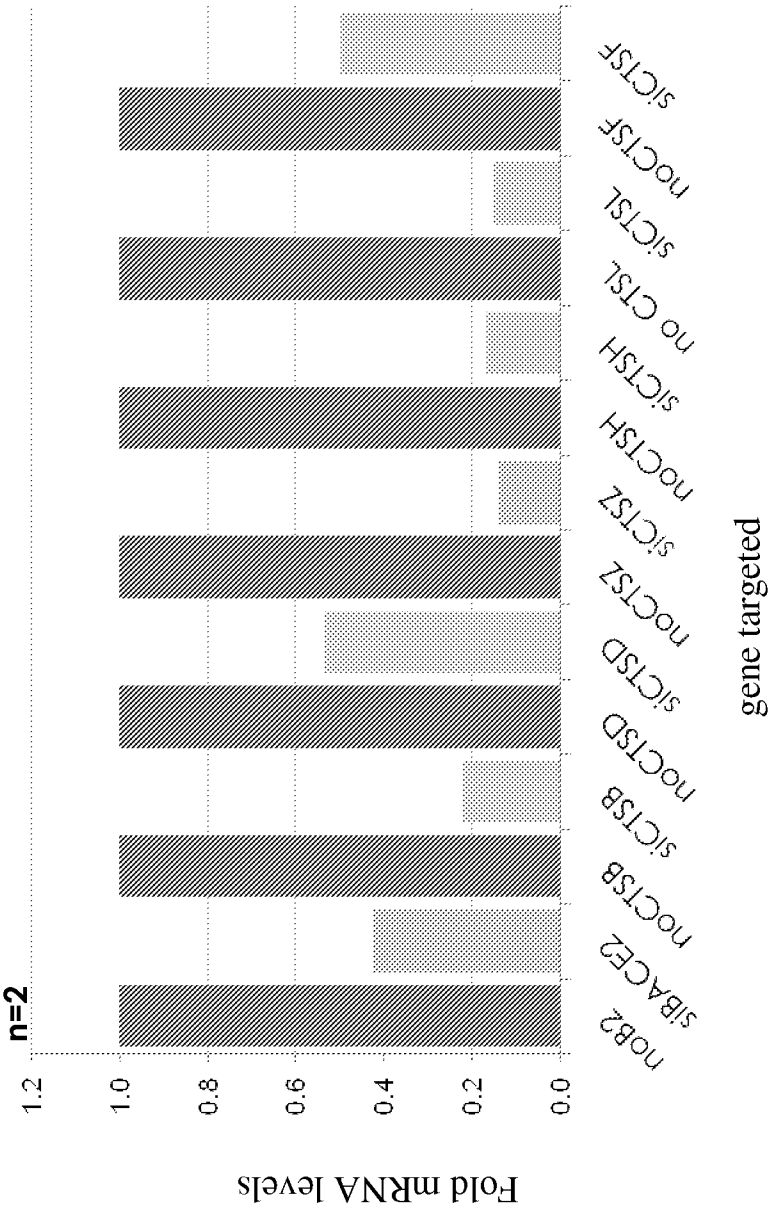

Fold mRNA levels
1.2
1.0
0.8
0.6
0.4
0.2
0.0
n=2
noB2
siBACE2
noCTSB
siCTSB
noCTSD
siCTSD
noCTSZ
siCTSZ
noCTSH
siCTSH
no CTSL
siCTSL
noCTSF
siCTSF
gene targeted

Fig. 6

Fig. 7A

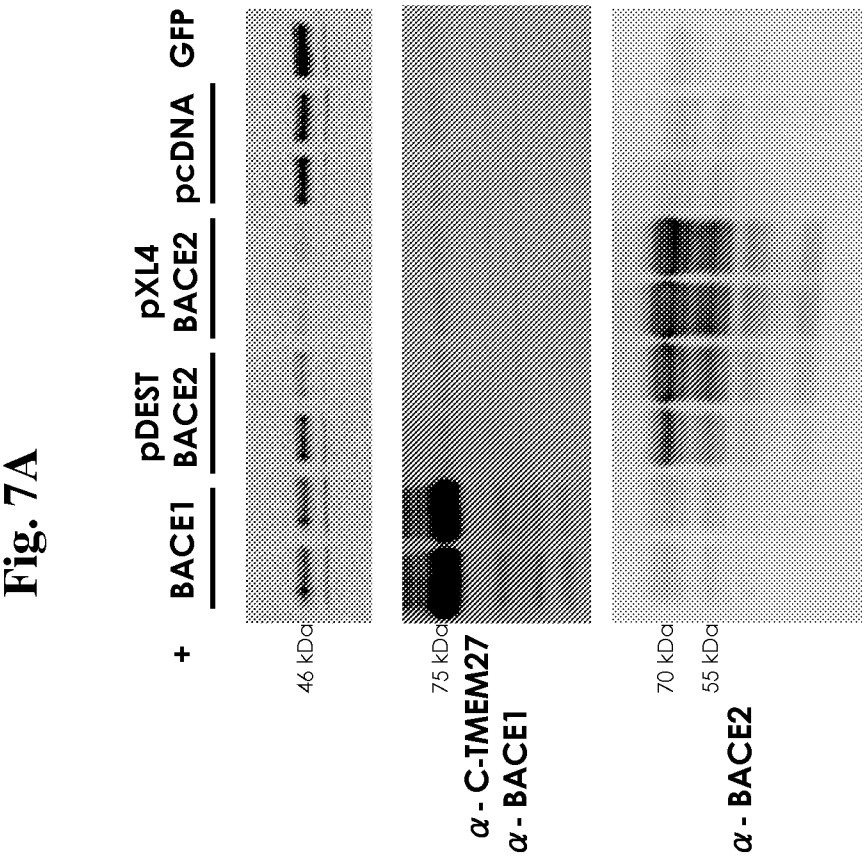


Fig. 7B

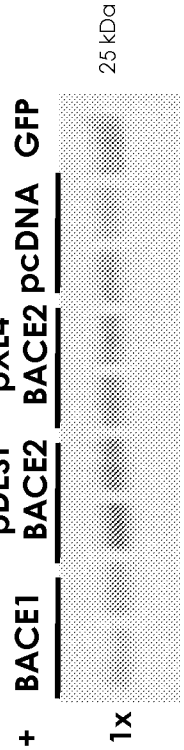


Fig. 7C

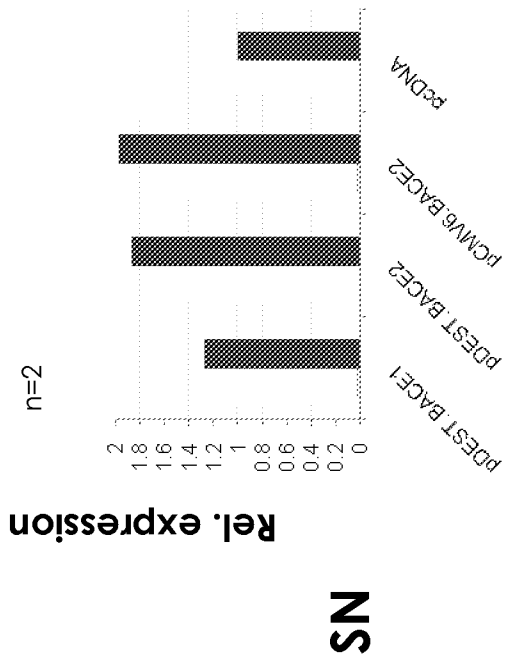


Fig. 8

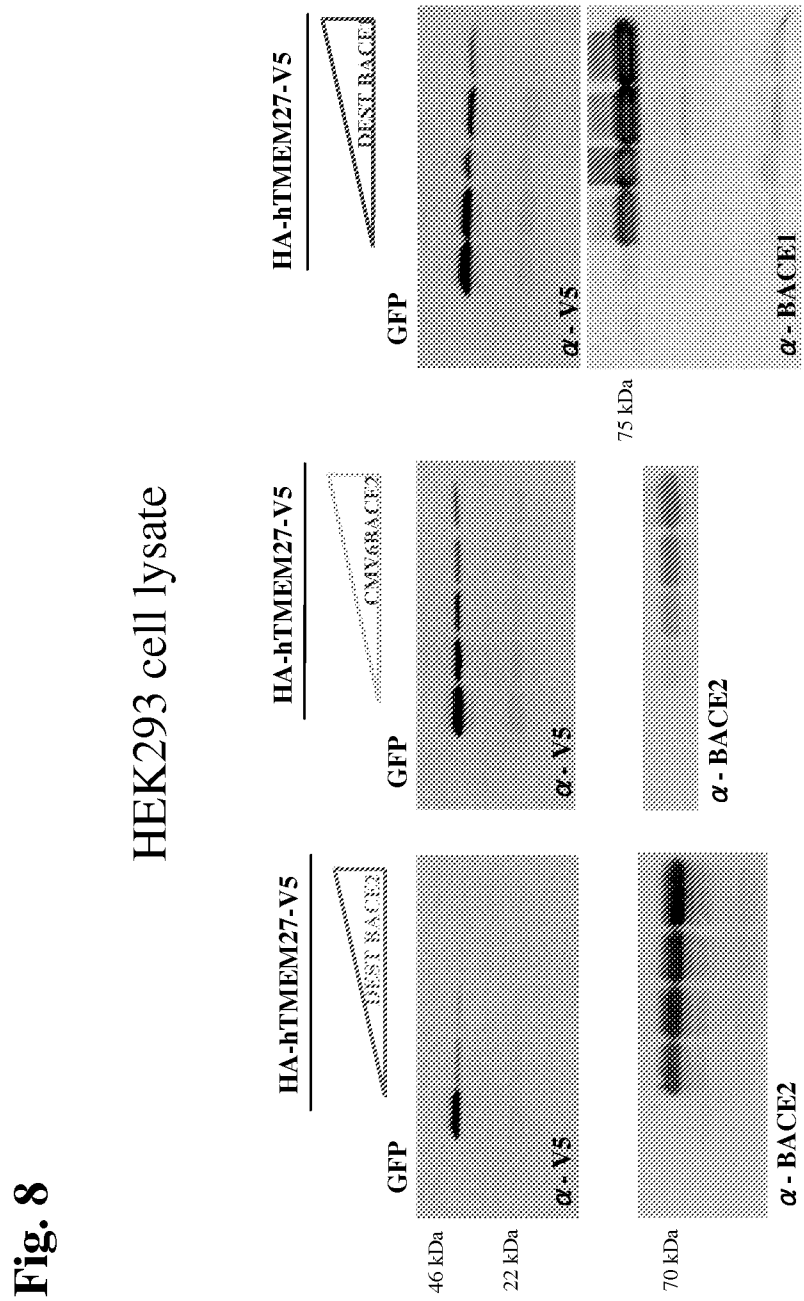

HEK293 cell lysate
HA-hTMEM27-V5
HSST BACE2
GFP
α - V5
46 kDa
22 kDa
α - BACE2
70 kDa
HA-hTMEM27-V5
CMV6BACE2
GFP
α - V5
α - BACE2
HA-hTMEM27-V5
BEST.BACE1
GFP
α - V5
75 kDa
α - BACE1

Fig. 9A

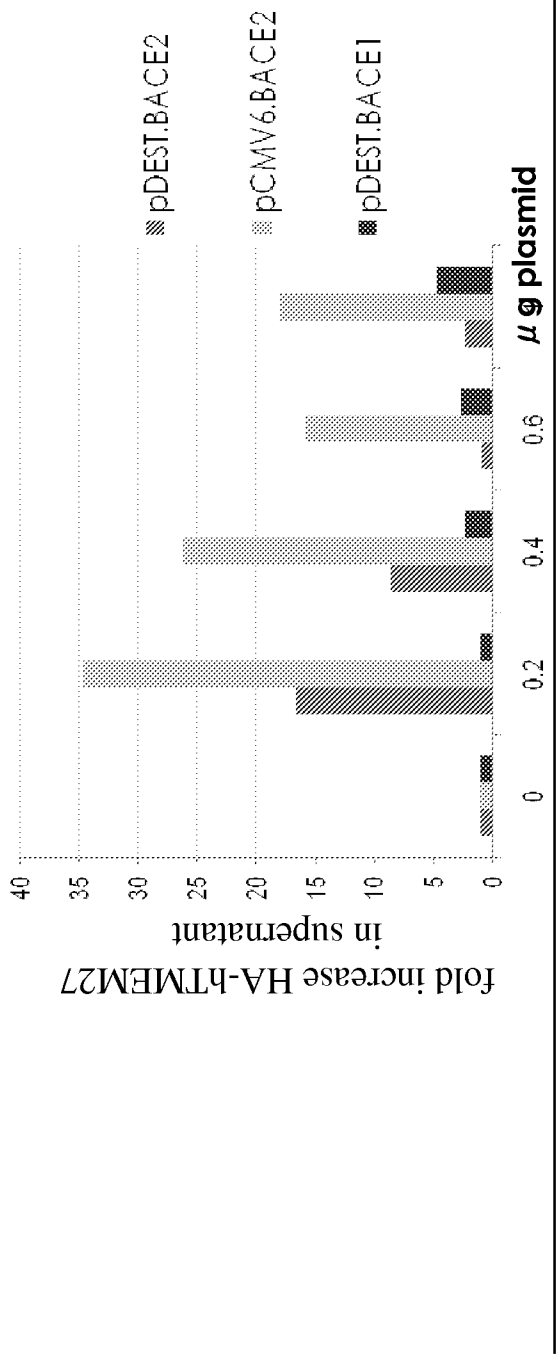
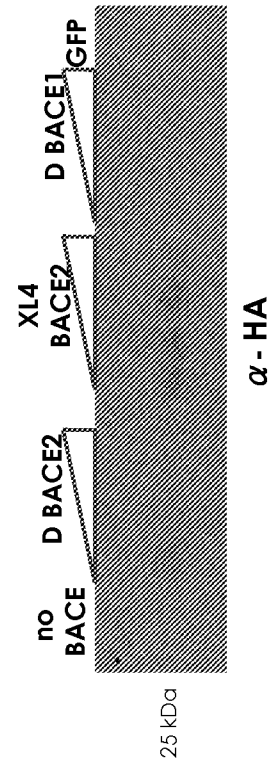

HEK293 cell supernatant
fold increase HA-hTMEM27 in supernatant
40
35
30
25
20
15
10
5
0
0
0.2
0.4
0.6
μg plasmid
pDEST.BACE2
pCMV6.BACE2
pDEST.BACE1

Fig. 9B


HA-TMEM27-V5
no BACE
D BACE2
XL4 BACE2
D BACE1
GFP
α - HA
25 kDa

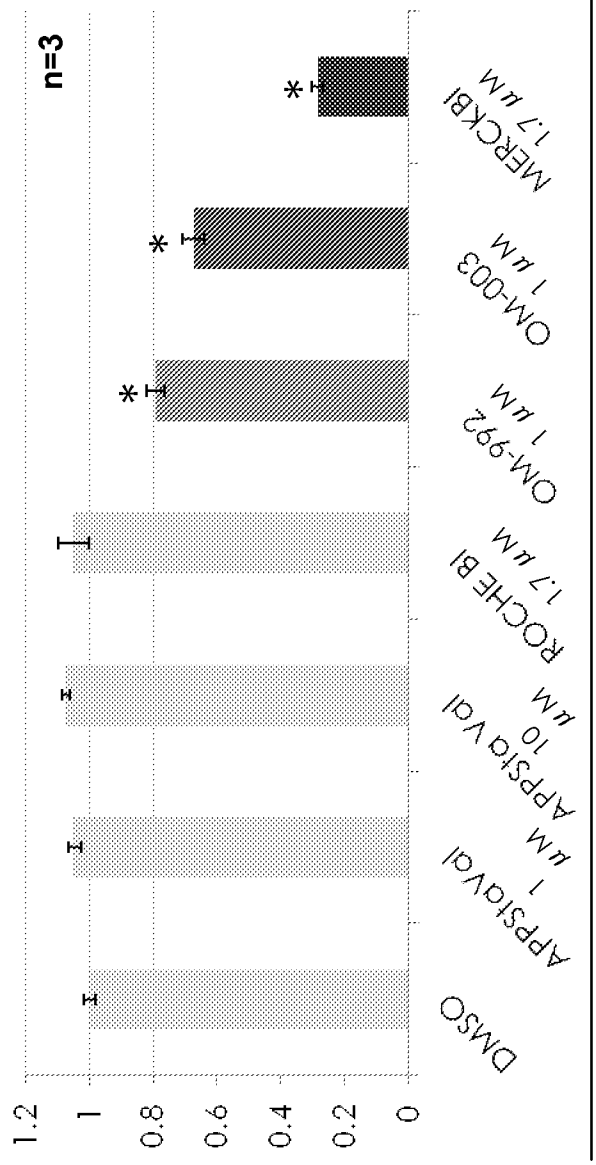


Fig. 10A

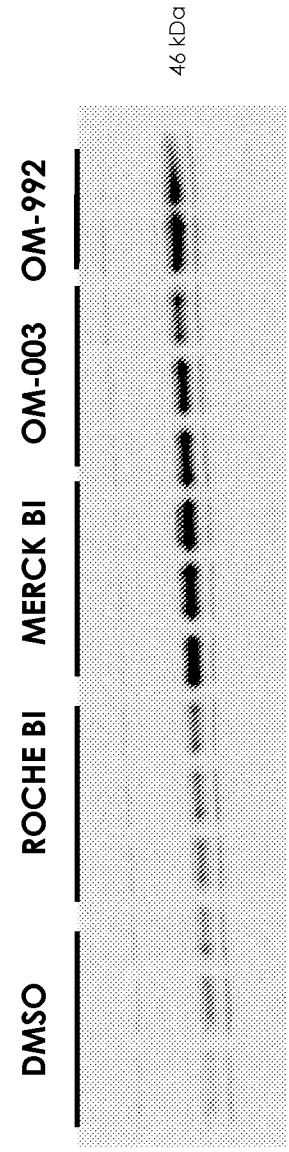
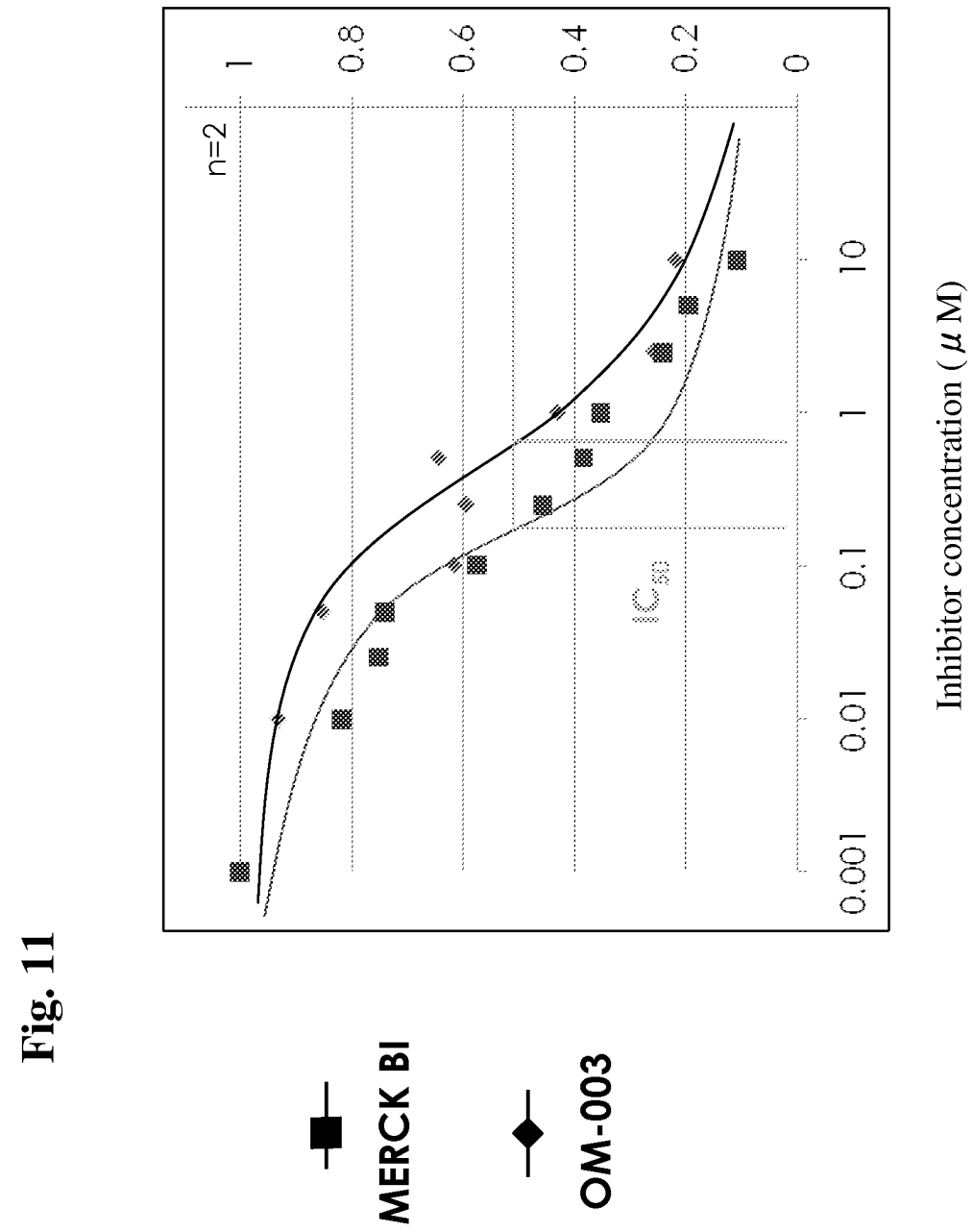


Fig. 10B

Fig. 11


Supernatant relative TMEM27
shedding inhibition
1
0.8
0.6
0.4
0.2
0
n=2
IC50
0.001
0.01
0.1
1
10
Inhibitor concentration (μM)
MERCK BI
OM-003

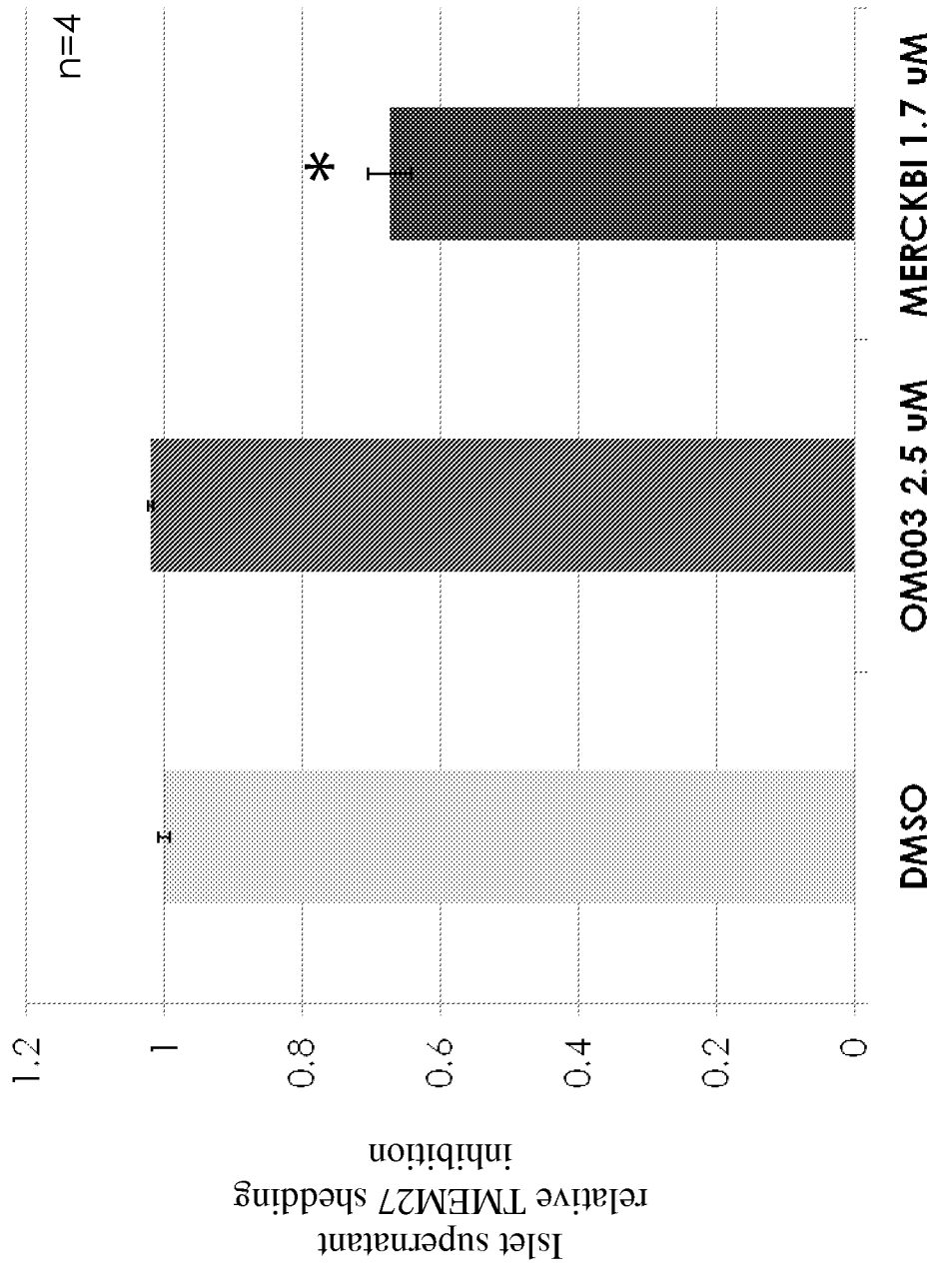

n=4
*
DMSO
OM003 2.5 uM
MERCKBI 1.7 uM
0
0.2
0.4
0.6
0.8
1
1.2
Islet supernatant
relative TMEM27 shedding
inhibition

Fig. 12

Fig. 13

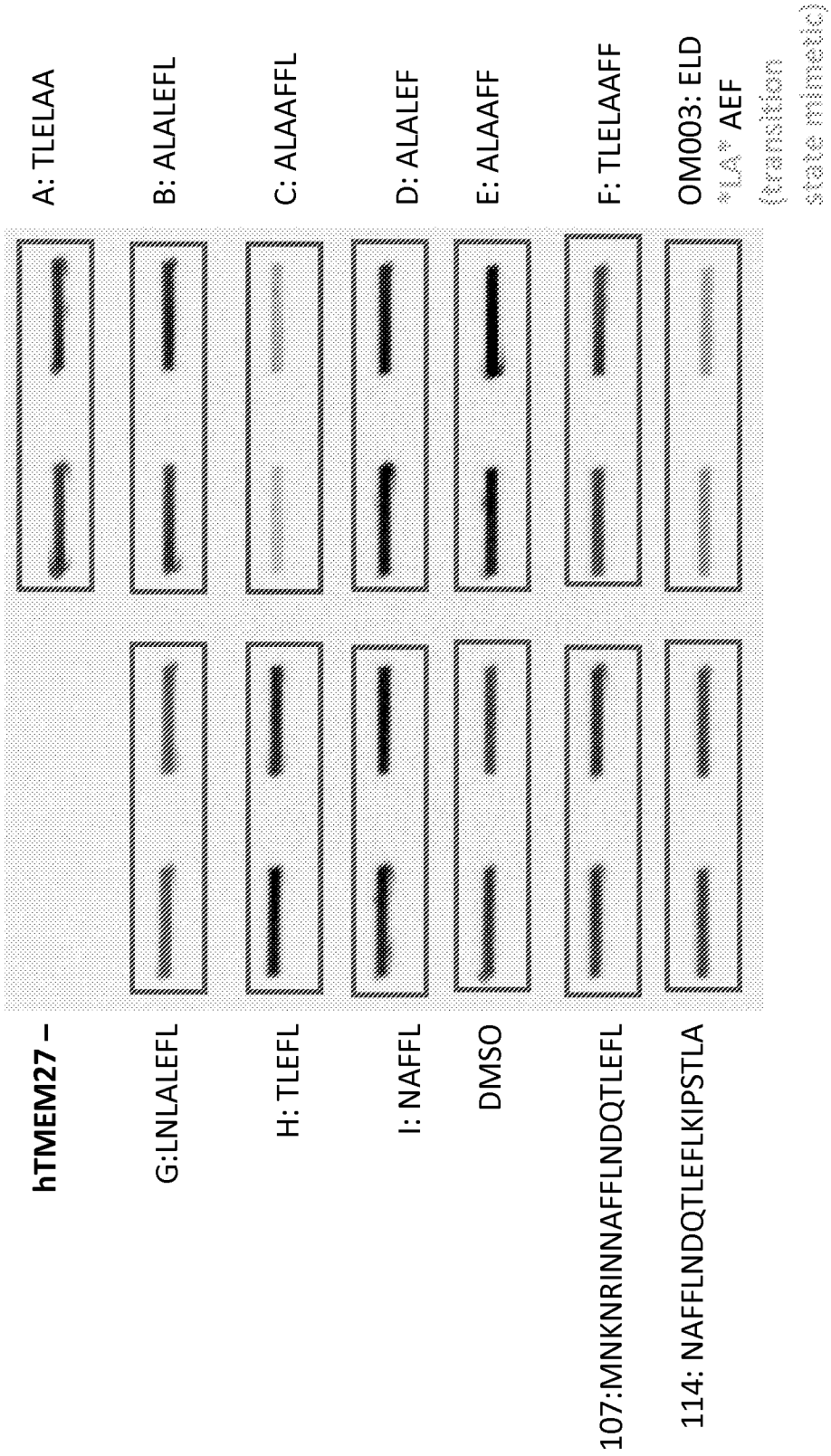
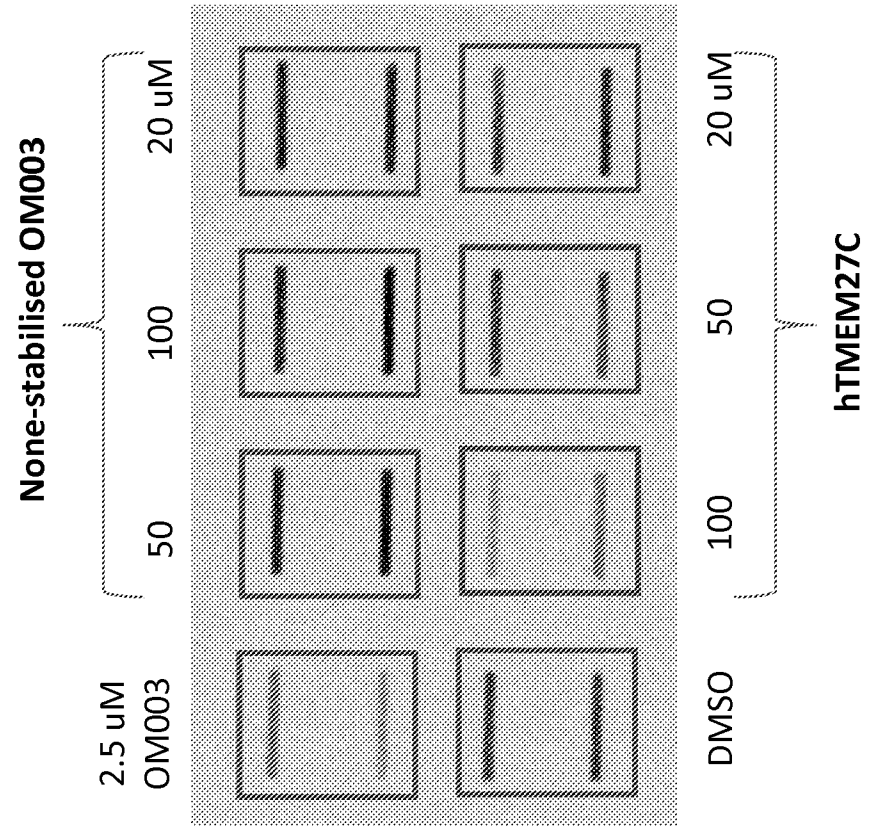

hTMEM27 –
G:LNLALEFL
H: TLEFL
I: NAFFL
DMSO
107:MNKNRINNAFFLNDQTLEFL
114: NAFFLNDQTLEFLKIPSTLA
A: TLELAA
B: ALALEFL
C: ALAAFFL
D: ALALEF
E: ALAAFF
F: TLELAAFF
OM003: ELD
LA AEF
(transition
state mimetic)

Fig. 14


None-stabilised OM003
2.5 uM OM003
50
100
20 uM
DMSO
100
50
20 uM
hTMEM27C

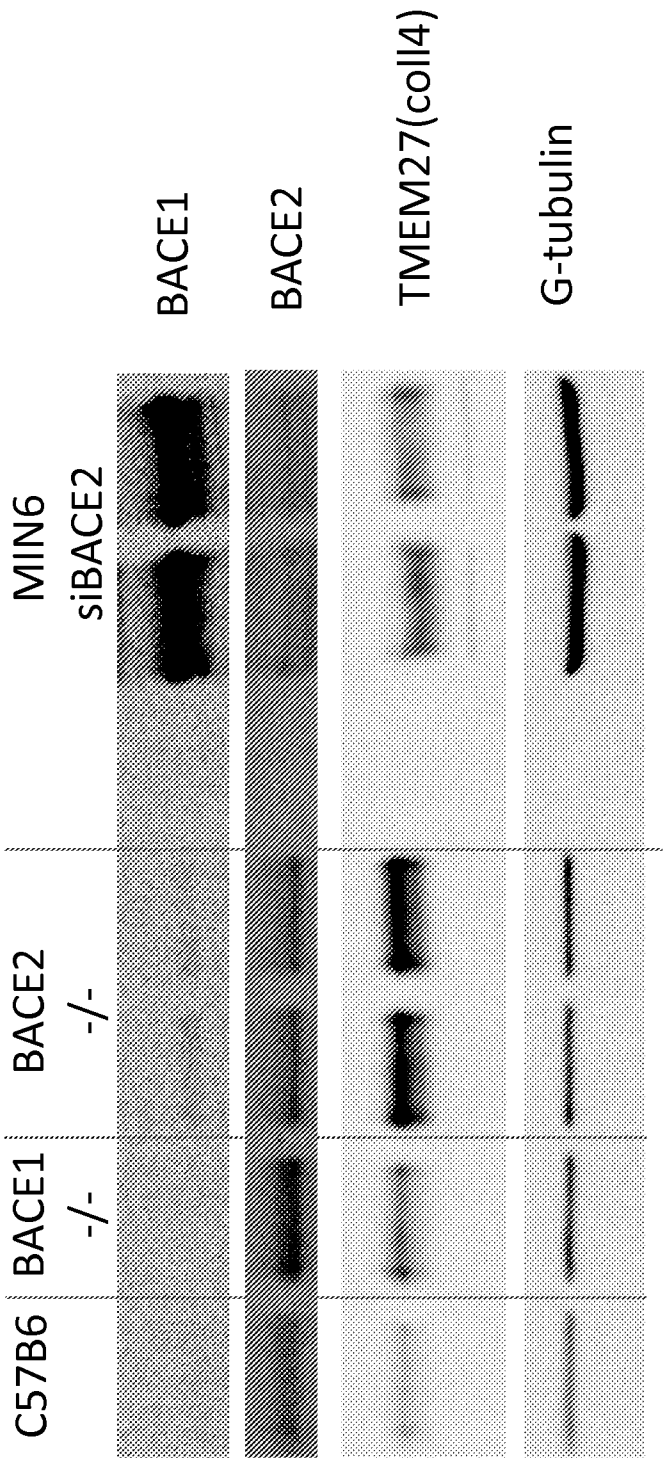

BACE1
BACE2
TMEM27(coll4)
G-tubulin
C57B6
BACE1 -/-
BACE2 -/-
MIN6 siBACE2

Fig. 15

Fig. 16A

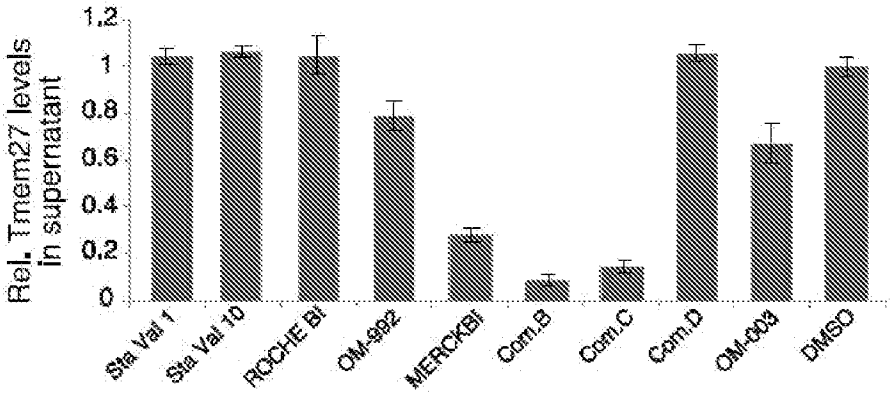


Fig. 16B

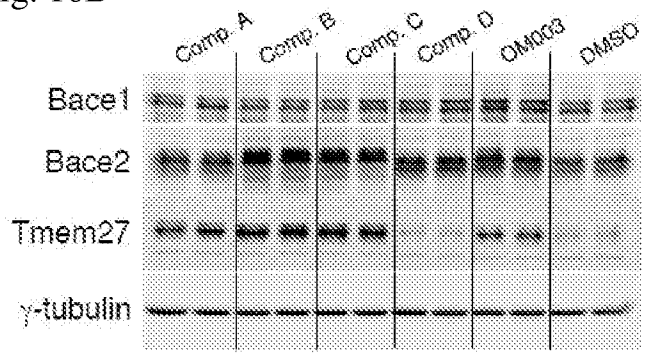


Fig. 16C

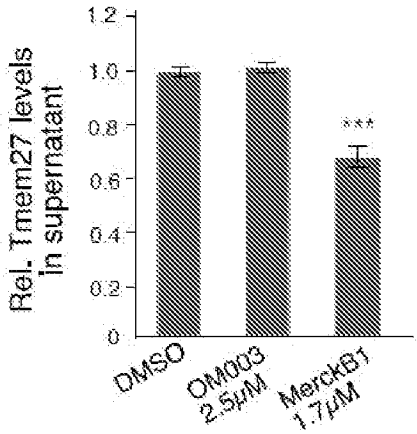


Fig. 16D

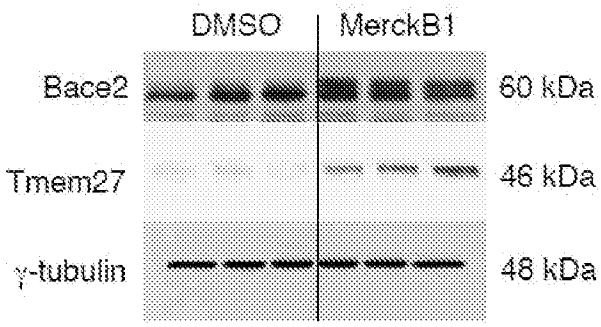


Fig. 17A

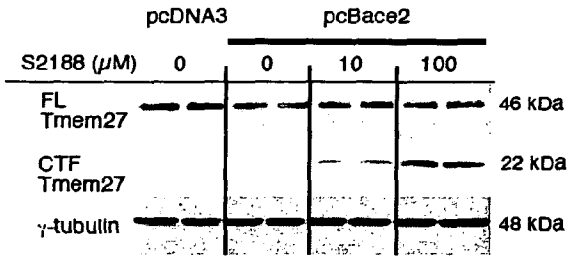


Fig. 17B

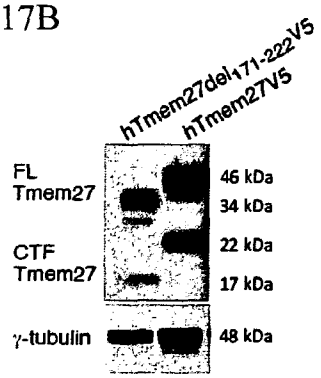


Fig. 17C

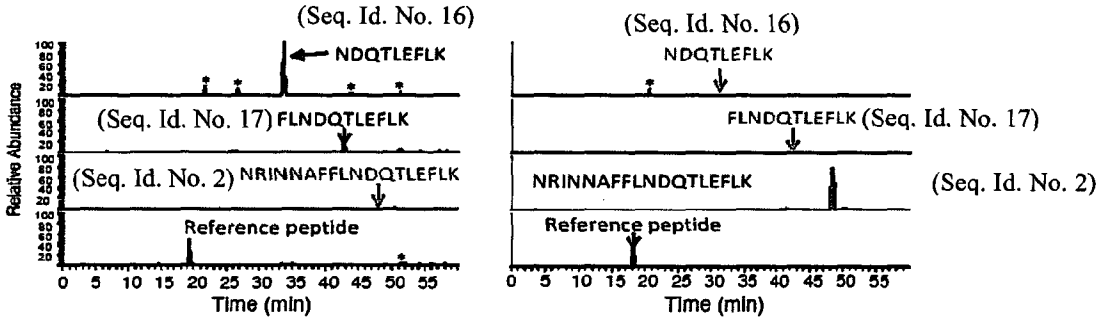


Fig. 17D

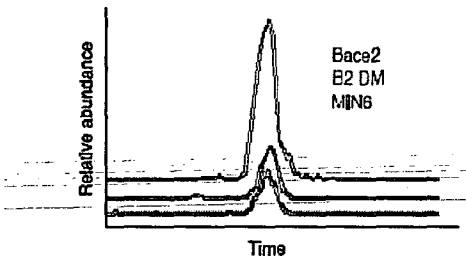


Fig. 17E

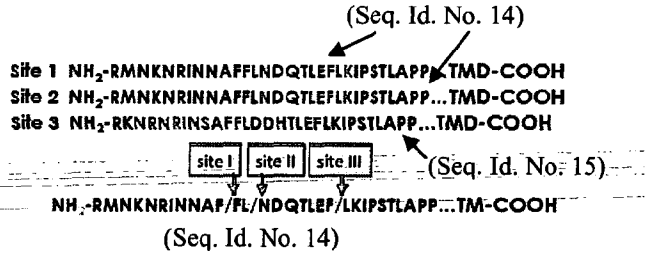


Fig. 17F

h TMEM27	NH_2-...RMNKNRINNAF / FL / NDQTLEF / LKIPSTLAPPMDPSVPI-TMD...COOH	(Seq. Id. No. 5)
m TMEM27	NH_2-...RKNRNRINSAF / FL / DDHTLEF / LKIPSTLAPPMEPSVPV-TMD...COOH	(Seq. Id. No. 6)
B. t TMEM27	NH_2-...RMNRNRINNAF / FL / NDQTLEF / LRIPSTLAPPTDPSVPI-TMD...COOH	(Seq. Id. No. 7)
X.t TMEM27	NH_2-...RNERNRINSAF / LL / DDKTLEF / VQIPPTLAPATQTSSSS-TMD...COOH	(Seq. Id. No. 8)
D. r TMEM27	NH_2-...RQSKHRINNAF / LL / SDMTLEF / VGVPPTLAVPIQYNTPP-TMD...COOH	(Seq. Id. No. 9)
BACE2 prodomain	NH_2-... PAERHADGL / ALALEPALASPAGAANF / L / AMVD...TMD...COOH	(Seq. Id. No. 10)
APP SWEDISH MUTANT	NH_2-... SEVL / DAEFRHDSGYEVHHQK / LVF / F / AEDVGSNK-TMD...COOH	(Seq. Id. No. 11)
APP	NH_2-... SEVKMDAEFRHDSGYEVHHQK / LVF / F / AEDVGSNK-TMD...COOH	(Seq. Id. No. 12)
IL-1R2	NH_2-...LEVVHNTLSF / QTLRTTVKEASSTFS-TMD...COOH	(Seq. Id. No. 13)

Fig. 18A

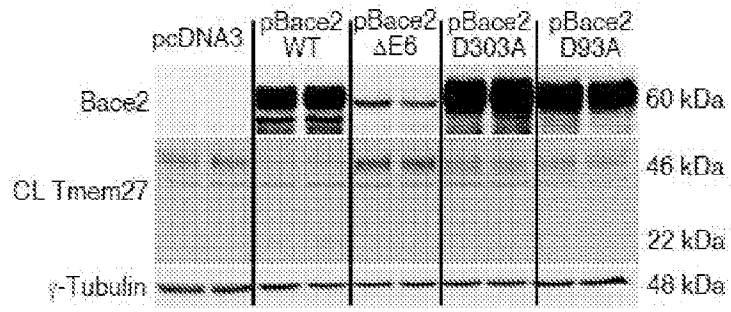


Fig. 18B

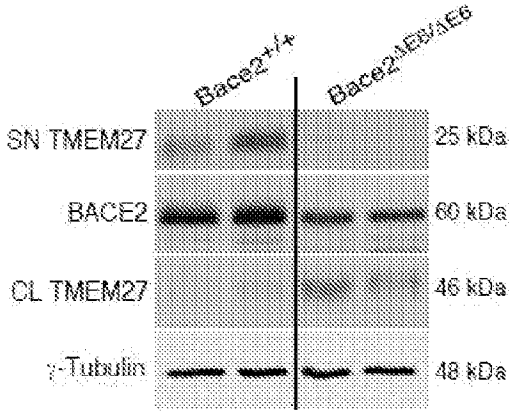


Fig. 18C

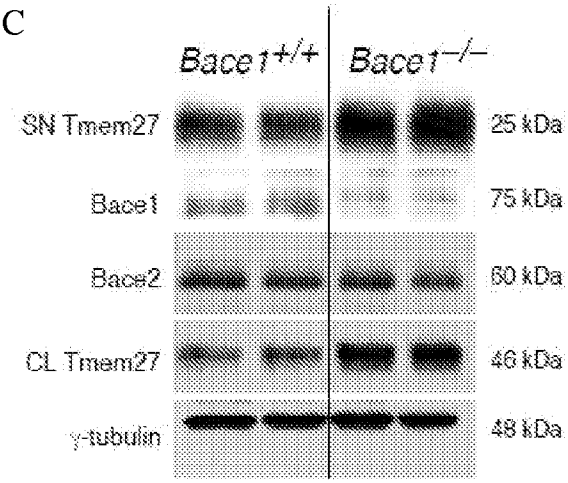


Fig. 18D

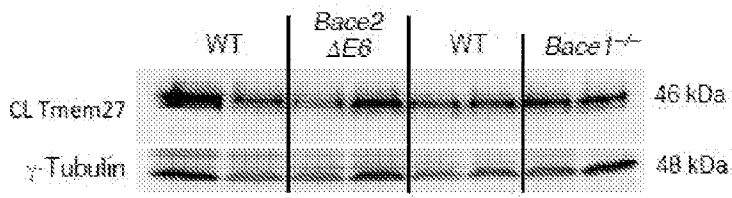


Fig. 19A

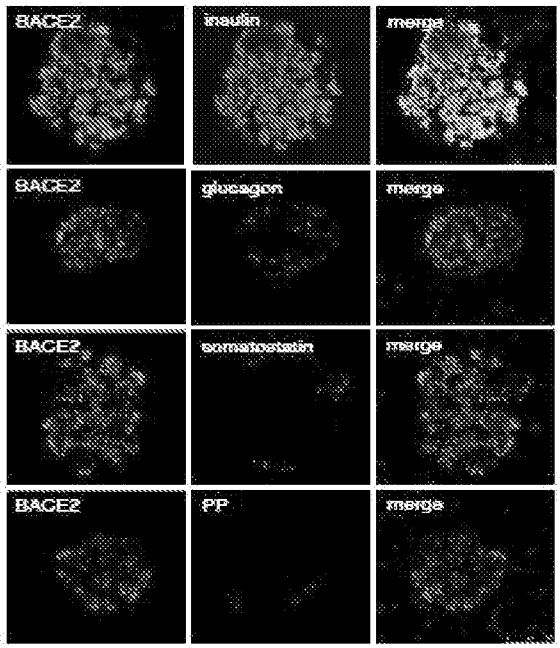


Fig. 19B

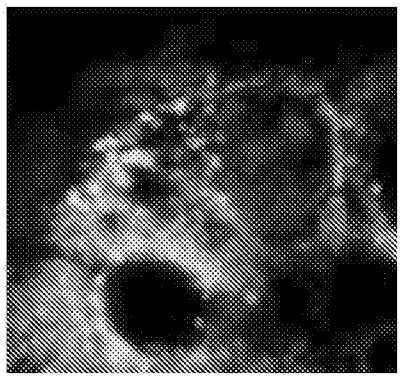


Fig. 19C

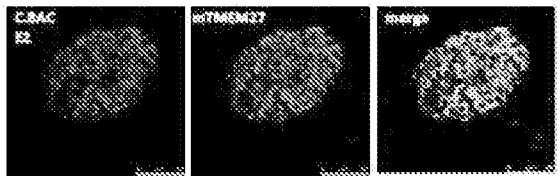


Fig. 19D

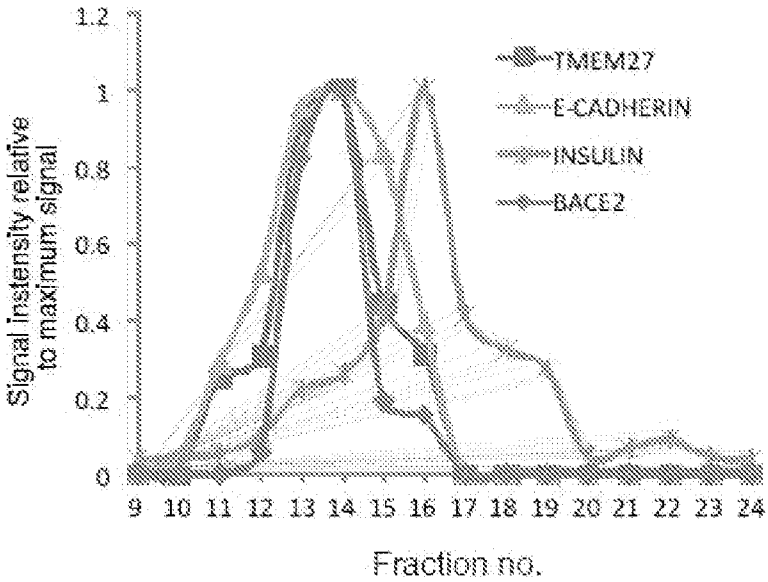


Fig.20

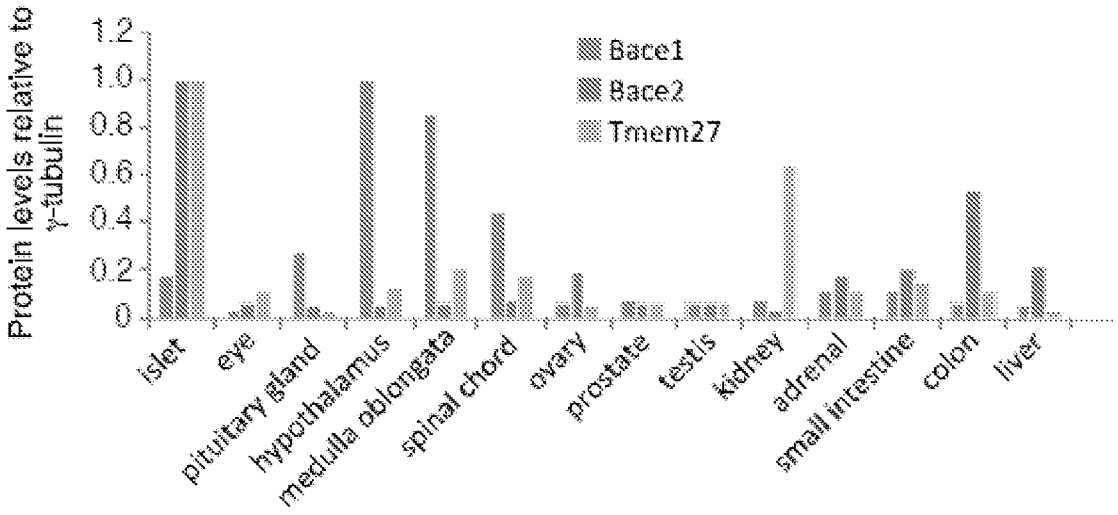

Protein levels relative to γ-tubulin
1.2
1.0
0.8
0.6
0.4
0.2
0
Bace1
Bace2
Tmem27
islet
eye
pituitary gland
hypothalamus
medulla oblongata
spinal chord
ovary
prostate
testis
kidney
adrenal
small intestine
colon
liver

Fig. 21A

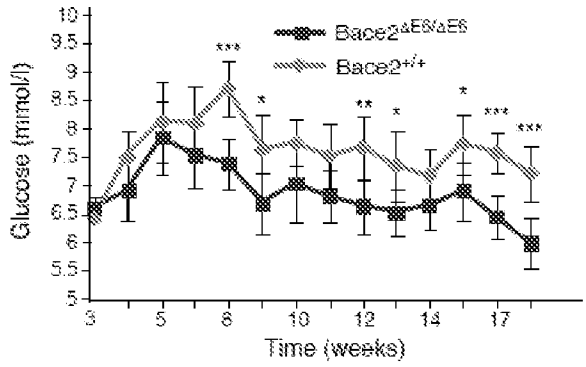


Fig. 21B

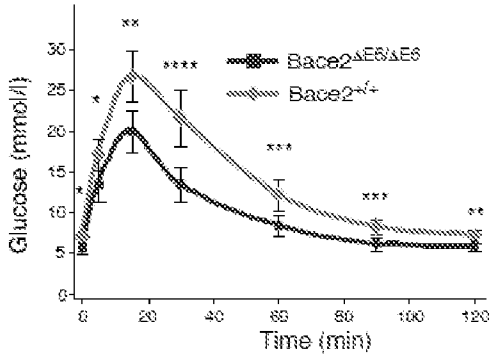


Fig. 21C

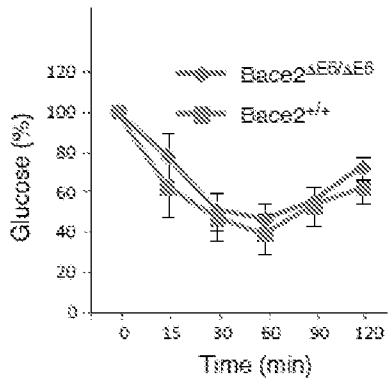


Fig. 21D

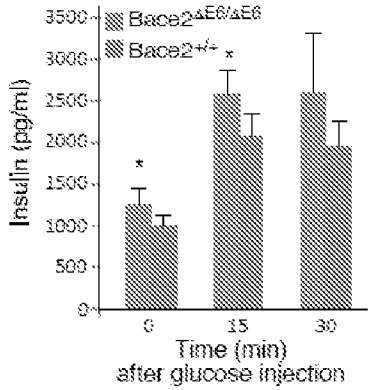


Fig. 21E

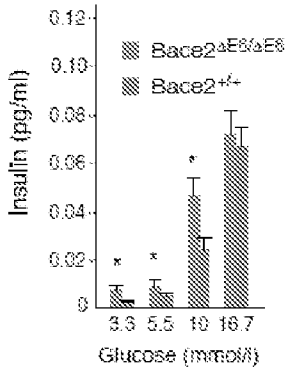


Fig. 21F

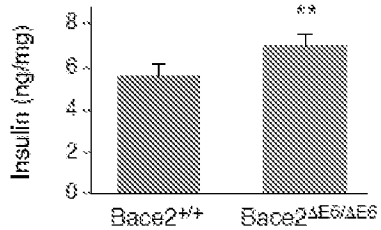


Fig. 21G

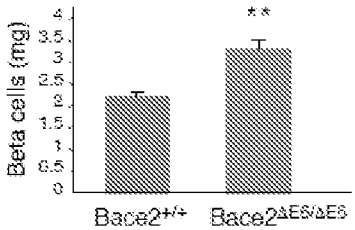
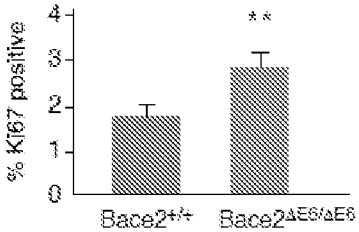


Fig. 21H



INTERNATIONAL SEARCH REPORT

International application No
PCT/EP2009/066151

A. CLASSIFICATION OF SUBJECT MATTER
INV. G01N33/68 C12N9/64 C07K14/705

According to International Patent Classification (IPC) or to both national classification and IPC

B. FIELDS SEARCHED

Minimum documentation searched (classification system followed by classification symbols)
G01N

Documentation searched other than minimum documentation to the extent that such documents are included in the fields searched

Electronic data base consulted during the international search (name of data base and, where practical, search terms used)
EPO-Internal, BIOSIS

C. DOCUMENTS CONSIDERED TO BE RELEVANT

Category*	Citation of document, with indication, where appropriate, of the relevant passages	Relevant to claim No.
A	WO 2006/133333 A2 (UNIV ROCKEFELLER [US]; STOFFEL MARKUS [US]; AKPINAR PINAR [US]) 14 December 2006 (2006-12-14) the whole document	1-12
A	AKPINAR PINAR ET AL: "Tmem27: A cleaved and shed plasma membrane protein that stimulates pancreatic beta cell proliferation" December 2005 (2005-12), CELL METABOLISM, VOL. 2, NR. 6, PAGE(S) 385-397 URL , XP002567279 ISSN: 1550-4131 the whole document in particular on page 394, left column, lines 33-36, and the last sentence on said page	1-12

-/--

[X] Further documents are listed in the continuation of Box C.

[X] See patent family annex.

* Special categories of cited documents :

"A" document defining the general state of the art which is not considered to be of particular relevance

"E" earlier document but published on or after the international filing date

"L" document which may throw doubts on priority claim(s) or which is cited to establish the publication date of another citation or other special reason (as specified)

"O" document referring to an oral disclosure, use, exhibition or other means

"P" document published prior to the international filing date but later than the priority date claimed

"T" later document published after the international filing date or priority date and not in conflict with the application but cited to understand the principle or theory underlying the invention

"X" document of particular relevance; the claimed invention cannot be considered novel or cannot be considered to involve an inventive step when the document is taken alone

"Y" document of particular relevance; the claimed invention cannot be considered to involve an inventive step when the document is combined with one or more other such documents, such combination being obvious to a person skilled in the art.

"&" document member of the same patent family

Date of the actual completion of the international search	Date of mailing of the international search report
8 February 2010	24/02/2010

Name and mailing address of the ISA/	Authorized officer
European Patent Office, P.B. 5818 Patentlaan 2 NL – 2280 HV Rijswijk Tel. (+31-70) 340-2040, Fax: (+31-70) 340-3016	Mauhin, Viviane

Form PCT/ISA/210 (second sheet) (April 2005)

INTERNATIONAL SEARCH REPORT

International application No
PCT/EP2009/066151

C(Continuation). DOCUMENTS CONSIDERED TO BE RELEVANT

Category*	Citation of document, with indication, where appropriate, of the relevant passages	Relevant to claim No.
A	VASSAR R: "The beta-secretase, BACE: A prime drug target for Alzheimer's disease" JOURNAL OF MOLECULAR NEUROSCIENCE, BIRKHAEUSER, CAMBRIDGE, MA, US, vol. 17, no. 2, 1 October 2001 (2001-10-01), pages 157-170, XP009023186 ISSN: 0895-8696 the whole document	1-12
A	ESLER WILLIAM P ET AL: "A portrait of Alzheimer secretases: New features and familiar faces" 24 August 2001 (2001-08-24), SCIENCE (WASHINGTON D C), VOL. 293, NR. 5534, PAGE(S) 1449-1454 , XP002567280 ISSN: 0036-8075 the whole document	1-12
A	STACHEL S J ET AL: "STRUCTURE-BASED DESIGN OF POTENT AND SELECTIVE CELL-PERMEABLE INHIBITORS OF HUMAN .BETA.-SECRETASE (BACE-1)" JOURNAL OF MEDICINAL CHEMISTRY, AMERICAN CHEMICAL SOCIETY, WASHINGTON, US, vol. 47, no. 26, 11 November 2004 (2004-11-11), pages 6447-6450, XP002393611 ISSN: 0022-2623 figure 2 first paragraph on page 6447	11
A	WO 2004/073630 A2 (ROSKAMP RES LLC [US]; PARIS DANIEL [US]; MULLAN MICHAEL J [US]) 2 September 2004 (2004-09-02) the whole document	11

INTERNATIONAL SEARCH REPORT

Information on patent family members

International application No
PCT/EP2009/066151

Patent document cited in search report	Publication date	Patent family member(s)	Publication date
WO 2006133333 A2	14-12-2006	CA 2611002 A1	14-12-2006
		EP 1896605 A2	12-03-2008
		JP 2009501002 T	15-01-2009
		SG 156683 A1	26-11-2009
WO 2004073630 A2	02-09-2004	AU 2004212965 A1	02-09-2004
		BR PI0407597 A	21-02-2006
		CA 2516259 A1	02-09-2004
		CN 1777436 A	24-05-2006
		EP 1596878 A2	23-11-2005
		JP 2006517979 T	03-08-2006